

A Comprehensive Review of Deforestation Monitoring Using Remote Sensing Imagery

Komathy C¹, Geraldine Bessie Amali D² *

¹ Research Scholar, School of Computer Science and Engineering, Vellore Institute of Technology,
Vellore – 632014, India

² Associate Professor, School of Computer Science and Engineering, Vellore Institute of
Technology, Vellore – 632014, India

Email-id : geraldine.amali@vit.ac.in *

ABSTRACT: Deforestation is a significant environmental challenge, with severe consequences like land degradation, biodiversity loss, and climate change. It is therefore important to monitor forest change to maintain ecological balance and avoid natural calamities, such as floods and landslides. Satellite remote sensing helps in observing changes in forest cover both spatially and temporally. This article offers an in-depth analysis of the primary elements in monitoring forest cover using remote sensing imagery. An extensive study on the different types of input data: optical, radar, and Light Detection and Ranging (LiDAR) imagery was conducted on bi-temporal and multi-temporal approaches with the emphasis in preprocessing techniques such as radiometric calibration and atmospheric correction to ensure data reliability. The comparison of pixel, object, and hybrid analytical approaches for capturing deforestation dynamics was done. A detailed comparison of the various algorithmic approaches from traditional statistical methods to Machine Learning (ML) and Deep Learning (DL) models is provided. This includes Random Forest (RF), Support Vector Machines (SVM), Convolution Neural Networks (CNN), U-Net, and Transformer architectures. The models were compared and evaluated based on their classification accuracy, computational efficiency, and generalization capabilities for both binary and multi-class change detection. This review will help researchers develop strategies to address deforestation and support sustainable forest management.

25 **Keywords:** Deforestation, satellite remote sensing, change detection, Deep Learning, SAR, bi-
26 temporal analysis

27 **1. Introduction:**

28 Forests play a vital role in preserving ecological balance and regulating the global carbon cycle.
29 Deforestation caused by the expansion of agriculture is now a leading environmental concern in the
30 world (J. N. Hansen et al., 2020)(M. C. Hansen et al., 2013). The loss of trees accelerates global
31 warming, reduces ecosystem resilience, and affects the entire planet(Chen et al., 2022)(Desclée et al.,
32 2013). The Reducing Emissions from Deforestation and Forest Degradation (REDD+) program for
33 preventing the cutting down of trees and the degradation of forest areas was introduced by the United
34 Nations Framework Convention on Climate Change (UNFCCC) (Arcanjo et al., 2016) with the
35 objective of forest area monitoring. This made the governments take three major preventive measures:
36 sustainable land use, forest management, and early detection of deforestation (J. N. Hansen et al.,
37 2020).

38 In recent years, remote sensing technologies have been extensively utilised for monitoring
39 deforestation due to their ability to cover large areas, low cost, and capacity to capture temporal data.
40 Satellites such as the Landsat series, Sentinel-2, and PlanetScope, along with sensors such as
41 Synthetic Aperture Radar (SAR) and LiDAR, help provide the spatial and spectral data required for
42 effective forest cover monitoring (Soto et al., 2022). Spatial and multispectral data gathered from
43 various sensors are used to detect changes in forest cover under different environmental conditions
44 (Pulella et al., 2020). However, manual image interpretation and pixel-based data analysis are very
45 slow, difficult to handle, and error-prone when working with highly varied landscapes (Bergamasco
46 et al., 2022)(Karishma et al., 2022). The application of traditional ML-based techniques for forest
47 cover monitoring has successfully increased classification accuracy, yet they rely heavily on manual
48 feature engineering and struggle with complex forest structures.(Nguyen Trong et al., 2020)(Brovelli
49 et al., 2020). DL-based models such as CNNs, U-Net, DeepLabv3+, and transformers learn
50 hierarchical, spatial, and temporal features automatically, thereby reducing the need for extensive

51 preprocessing (Adarme et al., 2020)(de Bem et al., 2020)(Rakshit et al, 2018). Image segmentation
52 techniques have enabled an accurate, clear determination of deforested areas by separating forest and
53 non-forest classes (Selvaraj & Amali, 2023)(Rash et al., 2023). Cloud computing platforms like
54 Google Earth Engine (GEE) now support the processing of large amounts of data in less time (Rakshit
55 et al, 2018)(Karmoude et al., 2025)(Y. Zhang et al., 2024).

56 Numerous studies have been conducted on monitoring deforestation, yet many of them lack a
57 thorough comparative analysis, especially on the combination of data types, processing levels, and
58 detection strategies (Pulella et al., 2020)(Bergamasco et al., 2022). Furthermore, there is a shortage
59 of benchmark studies assessing ML and DL models in different ecosystems and over various time
60 periods (de Bem et al., 2020). These gaps highlight the need for a systematic review that examines
61 both traditional and modern approaches, identifies challenges, and outlines future directions. This
62 review aims to provide a systematic analysis of the various deforestation monitoring techniques.

63 **Key Objectives:**

- 64 • To examine how different satellite data sources, optical, SAR, LiDAR, and hyperspectral,
65 contribute to bi-temporal and multi-temporal monitoring of forest cover, and highlight their
66 relative strengths in diverse environmental settings.
- 67 • To evaluate the role of the preprocessing steps, including radiometric and atmospheric
68 correction, co-registration, and spectral index generation, and to assess how these procedures
69 influence change detection outcomes.
- 70 • To compare a pixel-based, object-based, and hybrid analytical approaches for detecting forest
71 changes in landscapes with varying spatial complexity.
- 72 • To critically assess traditional techniques, ML algorithms, and DL models with respect to
73 accuracy, computational efficiency, robustness, and their ability to generalise across regions
74 and time periods.

- 75 • To investigate binary versus multi-class classification outputs for forest management
76 purposes.
- 77 • To identify persistent challenges related to data quality, temporal inconsistency, model
78 generalisation, and evaluation practices, and to propose future research directions for
79 developing scalable and reliable deforestation monitoring frameworks.

80 The rest of the paper is organized as follows: Literature collection strategy, deforestation
81 monitoring workflow and evolution of change detection techniques is presented in the rest of
82 section 1, followed by remote sensing data sources in section 2, preprocessing and data
83 preparation techniques in section 3 and feature extraction and spectral indices in section 4. The
84 complete analysis of change detection approaches with the benchmark datasets is presented in
85 section 5, followed by performance metrics and critical analysis of the various techniques based
86 on the output map in sections 6 and 7. Challenges, future directions and conclusion are presented
87 in sections 8 and 9.

88 **1.1 Literature Search and Selection Strategy**

89 Databases such as Web of Science, Scopus, IEEE Xplore that are widely revered in the research
90 community were used. Keyword searches with Boolean operators to combine terms such as
91 "deforestation monitoring," "deep learning," "change detection," and "SAR/LiDAR" was used.
92 The selection was done on peer-reviewed articles published between 2013 and 2026. Articles
93 lacking standardised performance metrics or those focused solely on non-forest land cover were
94 excluded. A total of 86 high-impact studies with primary focus on technical evolution and

regional applicability. A detailed flow diagram on the process followed is presented in Figure 1

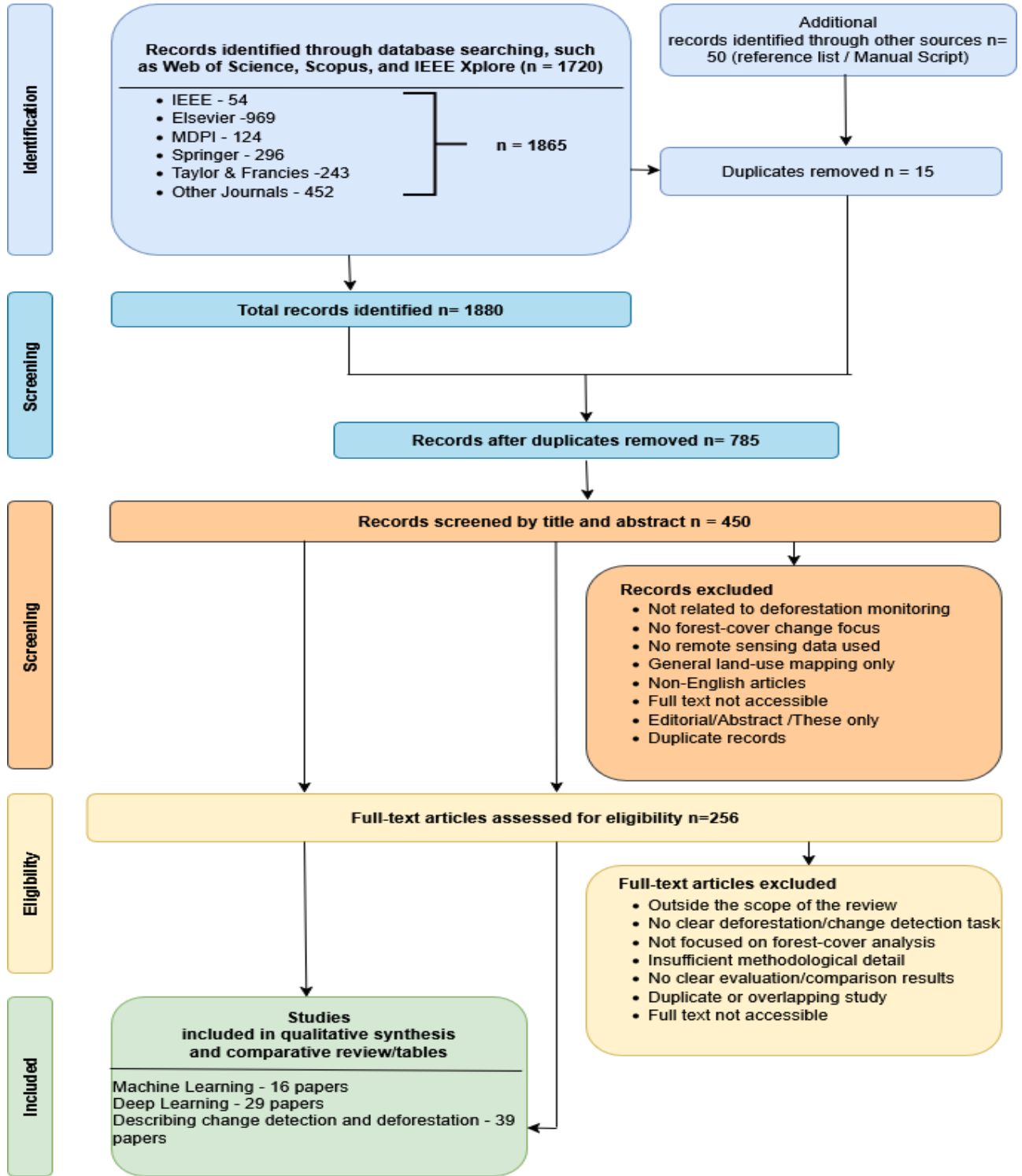
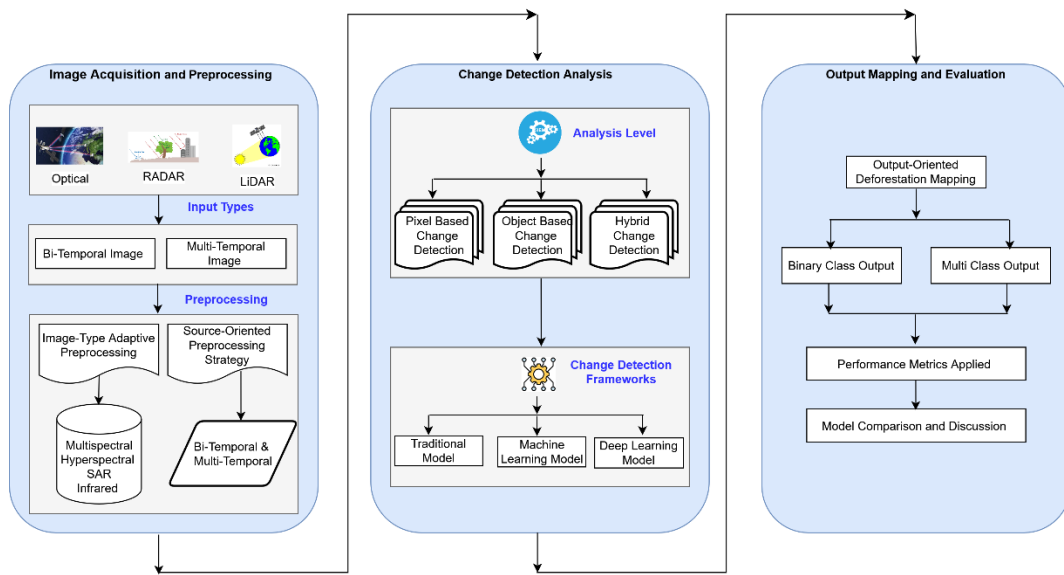


Figure 1. Flow diagram of the process used for study selection

1.2 Workflow for Deforestation Monitoring and Analysis



103

104

Figure 2. General framework for deforestation change detection from remote sensing data

105

Figure 2 illustrates the overall change detection workflow, which begins with image acquisition and

106

preprocessing. Data collected from different sensors, such as optical, radar, and LiDAR is then pre-

107

processed using image type adaptive preprocessing, which depends on the sensor, such as optical,

108

SAR, LiDAR, or source-oriented preprocessing, which depends on data characteristics, like

109

resolution and noise. The next stage in change detection is categorized into two parts, analysis level

110

and change detection framework. Pixel-based, object-based, and hybrid are the various methods of

111

analysis. Pixel-based change detection compares pixel values directly over time, object-based change

112

detection works on image segmentation and hybrid change detection combines pixel and object-based

113

approaches. Change detection frameworks, consists of traditional techniques, ML, and DL. The final

114

stage is output mapping and evaluation. The output types are categorised into binary or multi-class

115

classification.

116 1.3 Evolution of Change Detection Techniques

117 Change detection techniques have evolved from simple human visual analysis to the application of
118 sophisticated ML and DL technologies. The chronological development of deforestation detection

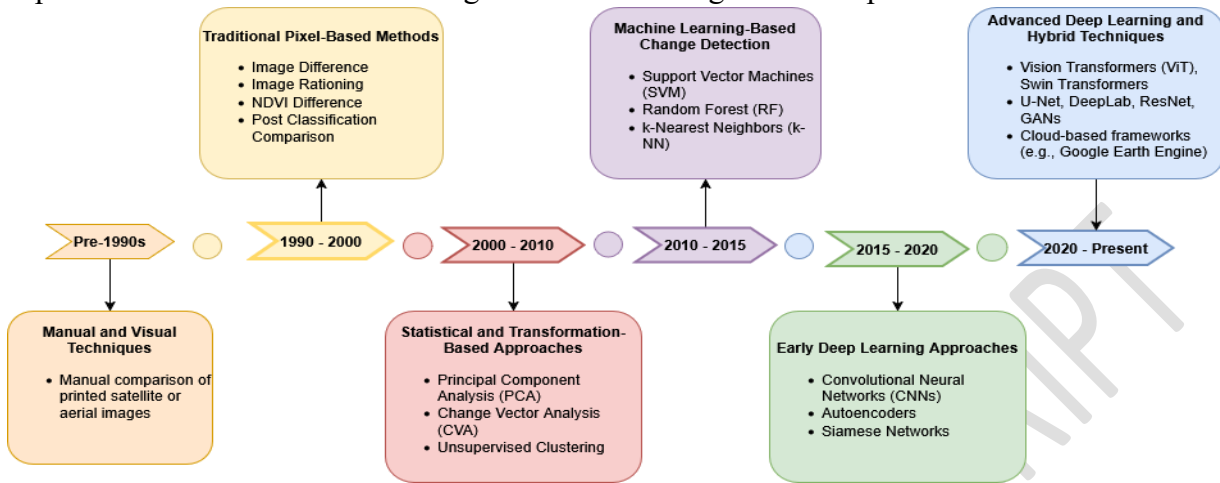
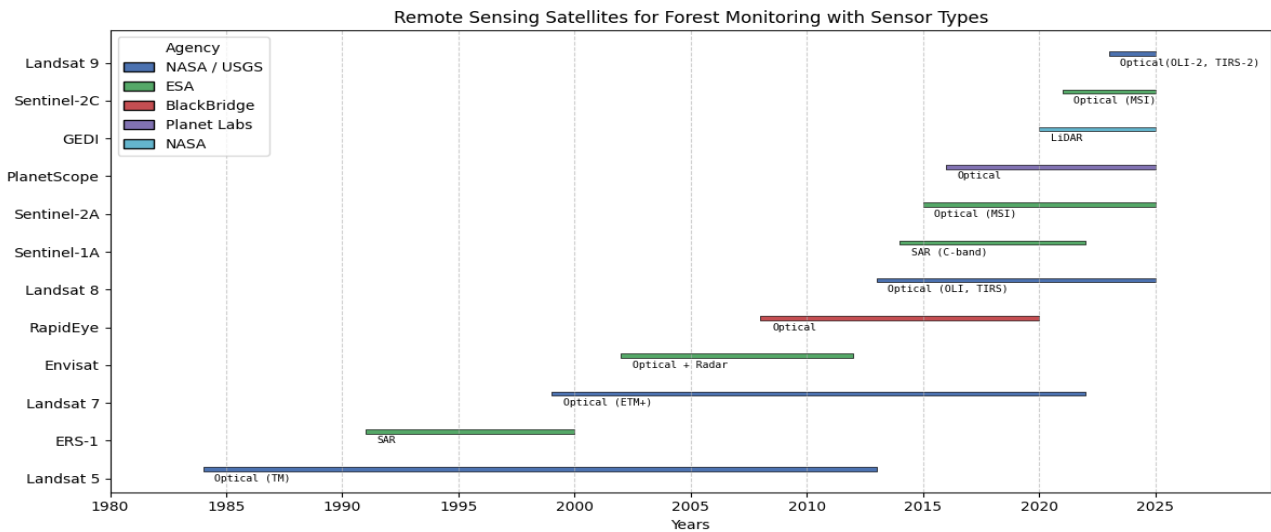


Figure 3. Evolution of deforestation change detection techniques over time

119 methods is shown in Figure 3. In the 1990s and earlier, visual methods were based on direct
120 comparisons of satellite or aerial photographs. The decade 1990-2000 saw the emergence of pixel-
121 based traditional techniques that made use of image differencing and Normalised Difference
122 Vegetation Index (NDVI) differencing (Nguyen Trong et al., 2020)(J. N. Hansen et al., 2020), image
123 ratioing, and post-classification comparison. In the years 2000-2010, statistical methods, namely
124 Principal Component Analysis (PCA), Change Vector Analysis (CVA) (Laurance et al.,
125 2014)Unsupervised clustering gained popularity. The period from 2010 to 2015 was a boom for
126 machine learning models, during which SVM, RF, and k-NN were the most widely used algorithms.
127 The years from 2015 to 2020 saw the growth of deep learning with CNN, autoencoders, and Siamese
128 networks. The last couple of years have seen the development hybrid models such as Vision
129 Transformers (ViT), Swin Transformers, U-Net, DeepLab, ResNet, and Generative Adversarial
130 Networks (GANs).

131 2. Remote Sensing Data Sources for Forest Change Detection

132 To accurately monitor deforestation datasets for the different spatial, spectral, and temporal aspects
133 of forest cover are needed (Brovelli et al., 2020)(Pacheco-Pascagaza et al., 2022).



134

135 **Figure 4.** Timeline of Major Remote Sensing Satellite Launches for Forest Monitoring

136 Figure 4 presents a timeline of major satellite missions used in forest monitoring from 1980 to 2030.

137 The chart distinguishes optical, SAR, and LiDAR sensors and highlights their operational periods and

138 responsible agencies. These missions together form the backbone of long-term, large-scale forest

139 observation programs and provide the valuable data needed to monitor forest cover.(Meiaraj,

140 2025)(Meiaraj, 2025)(Y. Zhang et al., 2024).

141 2.1. Optical Satellite Images

142 Optical sensors record reflected sunlight across visible, NIR(Near Infrared), and SWIR(Short-Wave

143 Infrared) wavelengths, used for the interpretation of vegetation vigour, soil exposure, and land cover

144 transitions(Karmoude et al., 2025). Multispectral and hyperspectral sensors provide high spectral

145 sensitivity, making them effective for identifying forest disturbances. Figure 5 (a),(b), and (c)

146 illustrate optical (RGB, panchromatic, and NIR) examples from the Thiruvannamalai district in India.

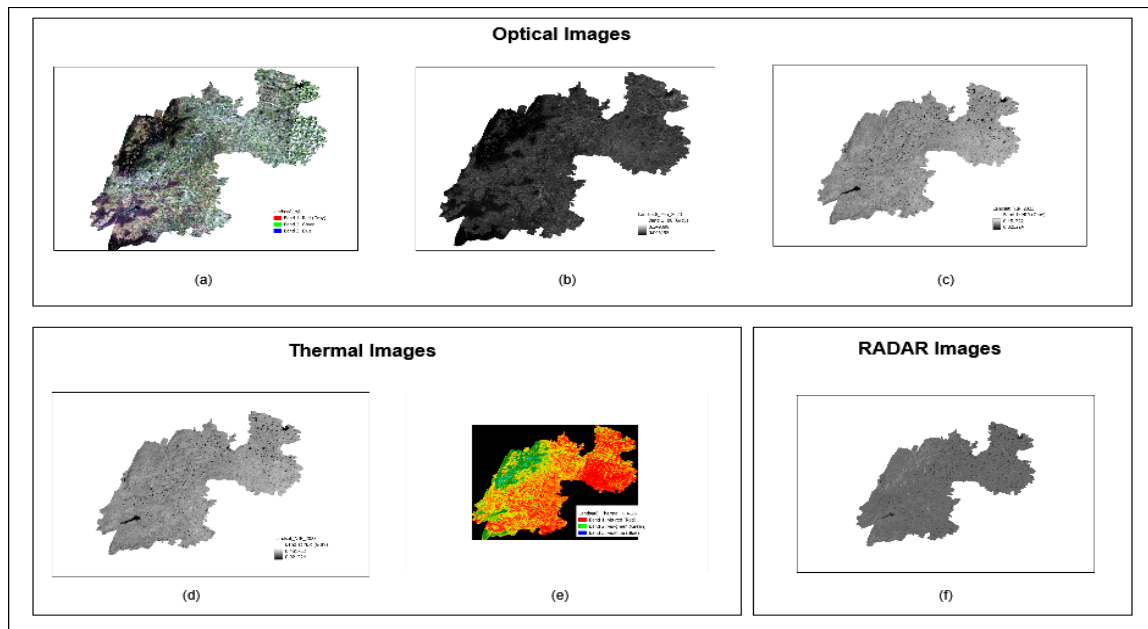
147 2.2 Thermal Images

148 Thermal imaging is used to spot forest fires, vegetation drought, and decay, and identify temperature

149 anomalies that are caused by the impact of cutting trees on local climate conditions (Nyamtseren et

150 al., 2025). Figures 5(d) and 5(e) present thermal imaging in Celsius and Kelvin, respectively.

151



152 2.3 Radar Image

153 Radar sensors, particularly SAR, emit microwave signals and receive backscattered signals from the
 154 Earth's surface, enabling consistent data acquisition regardless of time of day or weather conditions.
 155 SAR imagery covers structural forest analysis, degradation assessment, and detection of unauthorised
 156 logging activities(Neves et al., 2023)(Lucas et al., 2006). In Figure 4(f), a SAR image shows terrain
 157 unaffected by atmospheric conditions.

158 2.4 LiDAR

159 LiDAR calculates distances and generates highly detailed 3D models of vegetation through a series
 160 of laser pulses. This greatly assists in obtaining canopy height, biomass, and deforestation impact

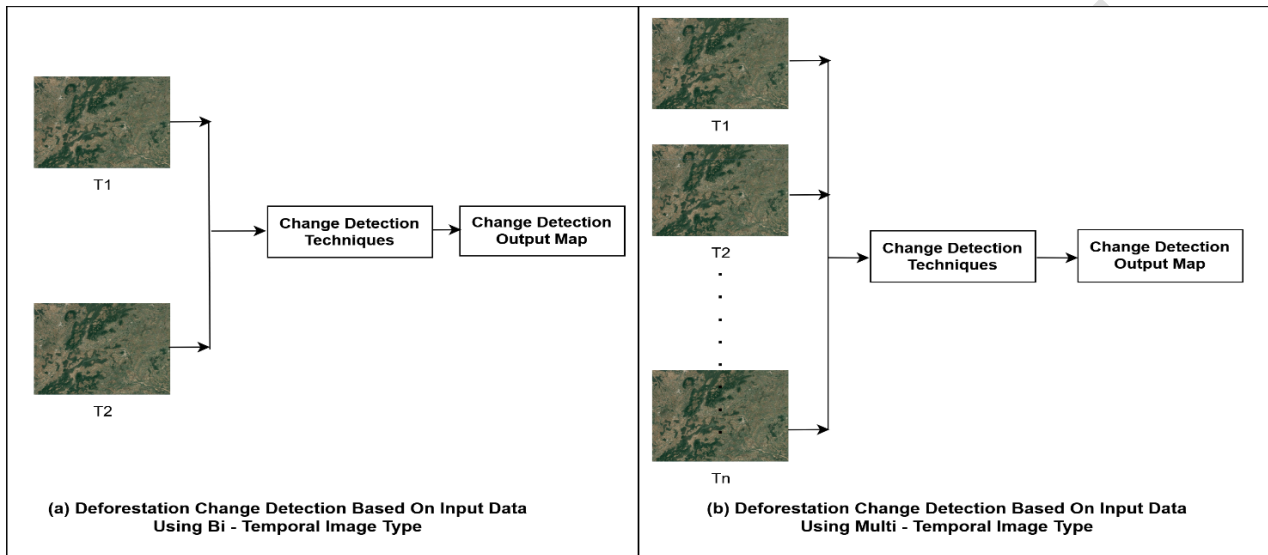
Figure 5. Comparative Satellite Imagery of Thiruvannamalai District (a) Optical RGB image (b) Panchromatic image (c) Near-Infrared (d) Thermal (Celsius) (e) Thermal (Kelvin) (f) SAR (Radar) image

161 estimation more accurately, particularly in areas of complex forest canopies (Boehm et al.,
 162 2013)(Lucas et al., 2006).

163 Different types of remote sensing images have distinctive characteristics that help monitor various
 164 aspects of deforestation. Optical imagery is good for showing changes in vegetation distribution and
 165 spectral characteristics, but it is affected by weather conditions. SAR guarantees reliable coverage
 166 over time and provides insights into its structure, which is crucial in tropical or monsoon climate

167 regions. LiDAR provides an exceptional level of detail for the evaluation of forest structure and
168 biomass, obtaining highly accurate results in the analysis of complex landscapes (Wagner et al.,
169 2023). The choice of inputs should depend on the aim of the research, geographic location, and the
170 required precision. Often, SAR is considered the most appropriate technique for forest monitoring.

171 2.5 Temporal Resolutions: Bi-Temporal vs Multi -Temporal



173 **Figure 6.** Deforestation change detection based on bi-temporal and multi-temporal image inputs.
174 Change detection can be performed using either bi-temporal or multi-temporal satellite images
175 (Figure 6). Bi-temporal data involves the comparison of two images taken at different times, thus
176 making it possible to observe if there is forest loss or not(Karmoude et al., 2025)(Reading et al.,
177 2024). However, multi-temporal datasets, through the integration of a series of images taken in
178 different periods, reveal long-term and seasonal trends (Rash et al., 2023)(Richardson et al., 2025).
179 Bi-temporal imagery clearly shows the sudden changes caused by logging or fire, whereas multi-
180 temporal imagery records the slow loss. DL architectures, such as 3D CNNs, ConvLSTMs, and
181 attention-based networks, utilize multi-temporal data to model complex spatiotemporal dependencies
182 (Parente et al., 2019). Thus, the combination of both architectures leads to better accuracy of
183 deforestation monitoring in various landscapes.

185 3. Preprocessing and Data Preparation

186 Preprocessing is a method that changes the raw satellite data into uniform and ready to be analyzed
187 datasets that can be used to monitor deforestation. A well-designed preprocessing pipeline is a key
188 factor in greatly enhancing feature reliability and model accuracy. The steps include eliminating
189 geometric and radiometric distortions, improving the alignment, and seasonal variations in the data.

190

191 3.1 Image Correction

192 The image correction procedure involves making the satellite images less affected by distorting
193 factors, namely atmospheric refraction, sensor limitations, and the Earth's curvature, to the least
194 possible extent. The accuracy of the analysis depends on this step.

- 195 • **Radiometric Correction:** The correction is performed by considering both the sensor's
196 sensitivity and atmospheric conditions to obtain the most accurate capture of the radiation that
197 has been reflected off the Earth's surface (Neves et al., 2023) (Cazzolla et al., 2025).
- 198 • **Geometric Correction:** The purpose of geometric correction is to make the satellite images
199 correspond to the actual ground coordinates by overcoming the sensor angles, Earth curvature,
200 and terrain distortion. This leads to the correct spatial interpretation of images (Desclée et al.,
201 2013).
- 202 • **Atmospheric Correction:** This correction minimises the effects of the atmosphere, such as
203 water vapour and aerosols, as well as scattering, to yield true surface reflectance. The
204 corrections performed in this manner increase the accuracy of the spectral data, which is
205 essential for both land cover mapping and longitudinal studies (Pulella et al., 2020).
- 206 • **Topographic Correction:**
207 Topographic variations in mountainous terrain create illumination imbalances that often
208 trigger false-positive deforestation detections due to spectral distortion. Applying correction

209 algorithms such as C-correction or Sun-Canopy-Sensor (SCS), and Minnaert correction
210 guided by Digital Elevation Models (DEM), helps normalise reflectance across sloped
211 surfaces. This preprocessing step improves the reliability of change detection by minimising
212 the influence of terrain-induced shadows(Y. Li et al., 2025)

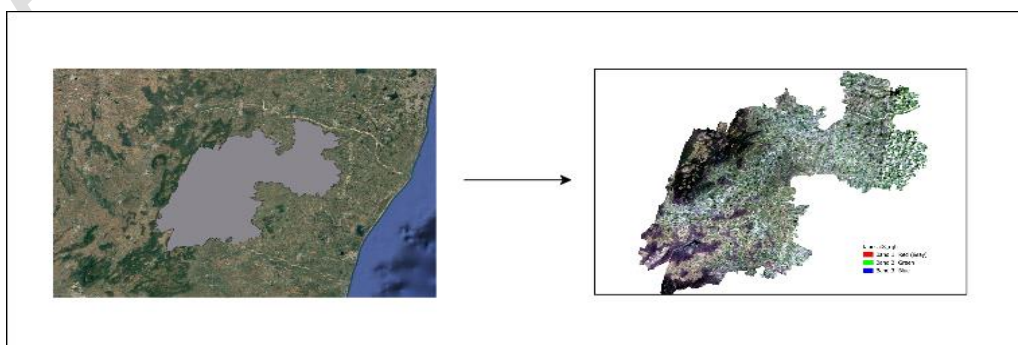
213 3.2 Co-registration

214 Co-registration is a crucial preprocessing step because it aligns satellite images taken at different
215 times of the same location on Earth. This makes it possible to observe the ground-truth features across
216 all images. Geometric unification is the key to reducing positional inaccuracies, thus increasing the
217 performance and reliability of change detection (Lucas et al., 2006).

218 3.3 Area of Interest (AOI)

219 AOI selection restricts analysis to a specific region, improving computational efficiency and ensuring
220 that only relevant forested areas are processed. Spatial masks derived from shapefiles of platforms
221 such as Google Earth Engine (GEE) and Quantum Geographic Information System (QGIS) are
222 commonly used(L. Gupta et al., 2025) (Atef et al., 2023). Figure 7 illustrates AOI extraction for the
223 Thiruvannamalai district in Tamil Nadu, India. This region is chosen for its forest cover.
224 Thiruvannamalai district has mixed terrain, including forest, agricultural, and rocky areas. It has high
225 spectral variability, similar signatures, such as confusion between dry forest and barren land making
226 land use class type separation difficult.

227



228

229 **Figure 7.** Extraction of Area of Interest (AOI) for Thiruvannamalai District

230 **3.4 Multi-Source Harmonization and Tiling**

231 When working with optical, radar, and thermal data, harmonization means that each data set is first
232 resampled, co-registered, and then normalised according to the characteristics of the sensor used.
233 Further steps, such as cloud masking, shadow removal, and radiometric calibration, will result in even
234 more consistent datasets. The processes of AOI masking and patch tiling are done to prepare the data
235 for ML/DL model input(Boehm et al., 2013)(Lucas et al., 2006).

236 **3.5. Preprocessing for Bi-Temporal vs Multi-temporal Inputs**

237 The preprocessing strategies for bi-temporal and multi-temporal inputs differ.

238 **3.5.1 Bi-Temporal Preprocessing Workflow**

239 Bi-temporal analysis uses images taken on different dates. Major steps are co-registration, radiometric
240 normalisation, and cloud/shadow masking indices, like NDVI or CVA, which are then extracted to
241 make the changes visible(Soto et al., 2022)(Oca et al., 2025)(Y. Zhou et al., 2023).

242 **3.5.2 Multi-temporal Preprocessing Workflow**

243 Multi-temporal datasets on the other hand go through an extensive preprocessing pipeline that
244 includes the steps of temporal stacking, gap-filling, and smoothing. These steps ensure that seasonal
245 signals are preserved and thus support models designed for long-term dynamics, such as LSTM(Long
246 Short Term Memory) or ConvLSTM networks(Ball et al., 2022)(Wagner, et al., 2023)(Cherif et al.,
247 2022)(Richardson et al., 2025). The next step is to extract meaningful spectral and spatial features
248 that highlight patterns of forest change.

249 **4. Feature Extraction and Spectral Indices**

250 After the preprocessing stage, feature extraction is the next important step in deforestation
251 monitoring, enabling significant inferences about land cover changes and dynamic representations.
252 Preprocessing serves to ensure data consistency, and while spatiotemporal alignment is achieved, it
253 fails to specifically highlight the characteristics of forest change. Spectral

254 Signatures such as NDVI, Enhanced Vegetation Index (EVI), and Normalised Burn Ratio (NBR) are
 255 very helpful for understanding features such as the amount and quality of vegetation, moisture
 256 content, and the severity of fire, all of which are important in determining the deforestation process.
 257 Feature extraction works based on spectral, spatial, and temporal
 258 characteristics, thus reducing the data dimensionality, but at the same time keeping
 259 the vital information. This process becomes the main factor that increases the input quality
 260 to the ML/DL models so they can be able to differentiate between slight vegetation changes
 261 and noise(Karmoude et al., 2025).

262 Furthermore, spectral indices derived from satellite reflectance band combinations are crucial for
 263 improving the detection of vegetation dynamics and deforestation studies. These indices enhance the
 264 spectral contrast between forest cover and deforestation, assisting in the accurate monitoring of forest
 265 loss during bi-temporal or multi-temporal imagery (L. Gupta et al., 2025)

266

$$NDVI = \frac{(NIR - Red)}{(NIR + Red)} \quad (1)$$

$$EVI = G \times \frac{(NIR - Red)}{(NIR + C_1 \times Red - C_2 \times Blue + L)} \quad (2)$$

$$SAVI = \frac{(NIR - Red)}{(NIR + Red + L)} \times (1 + L) \quad (3)$$

$$DVI = NIR - Red \quad (4)$$

$$NDWI = \frac{(Green - NIR)}{(Green + NIR)} \quad (5)$$

$$NDBI = \frac{(SWIR - NIR)}{(SWIR + NIR)} \quad (6)$$

$$MSAVI = \frac{2NIR + 1 - \sqrt{(2 \times NIR + 1)^2 - 8 \times (NIR - Red)}}{2} \quad (7)$$

$$VCI = 100 \times \frac{(NDVI - NDVI_{min})}{(NDVI_{max} - NDVI_{min})} \quad (8)$$

$$BAI = 1 - \frac{1}{(0.1 - Red)^2 + (0.06 - NIR)^2} \quad (9)$$

$$BSI = \frac{(SWIR - Red) - (NIR + Blue)}{(SWIR + Red) + (NIR + Blue)} \quad (10)$$

$$NDSI = \frac{(SWIR - NIR)}{(SWIR + NIR)} \quad (11)$$

267 where Near-Infrared (*NIR*), *Red*, *Green*, *Blue*, and Short-Wave Infrared (*SWIR*) represent the
 268 near-infrared, red, green, blue, and shortwave infrared reflectance bands, respectively, whereas *G*,
 269 C_1 , C_2 , and *L* denote empirical coefficients used in the EVI formulation.

270 Table 1 Common Spectral Indices Used in Deforestation Change Detection

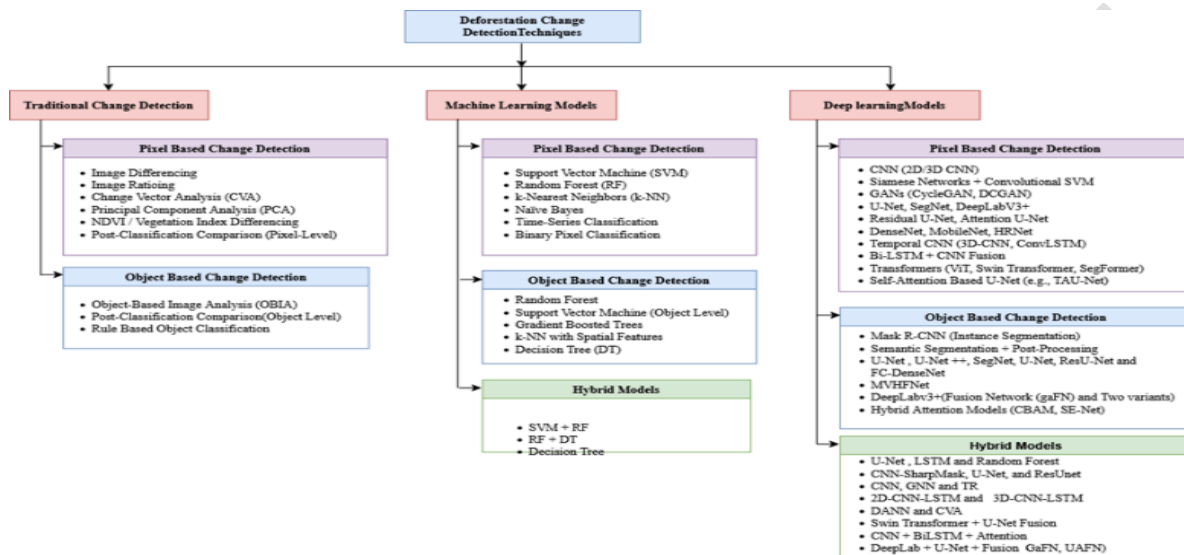
Index	Purpose
Normalized Difference Vegetation Index (NDVI) (Nguyen Trong et al., 2020)	Detects vegetation health and density, commonly used for forest loss assessment.
Enhanced Vegetation Index (EVI) (Potić et al., 2023)	Reduce atmospheric and soil background noise in dense vegetation areas.
Soil Adjusted Vegetation Index (SAVI) (K. Xu et al., 2021)	Compensates for soil brightness, effective in sparse vegetation zones.
Difference Vegetation Index (DVI) (J. N. Hansen et al., 2020)(K. Xu et al., 2021)	Quantifies vegetation density variation pre/post deforestation
Normalized Difference Water Index (NDWI) (Masolele et al., 2022)(Moni et al., 2025)	Identifies water presence and moisture variation in vegetation
Normalized Difference Built-up Index (NDBI) (Atef et al., 2023)	Detects built-up or developed areas replacing forest cover
Modified SAVI (MSAVI) (Atef et al., 2023)	Enhance vegetation detection in low-cover regions by minimizing soil influence
Vegetation Condition Index (VCI) (J. N. Hansen et al., 2020)	Tracks the temporal vegetation decline for monitoring degradation
Burned Area Index (BAI) (Atef et al., 2023)	Identifies fire-affected forest areas, indicating degradation
Bare Soil Index (BSI) (Masolele et al., 2022)	Detects bare soil linked to deforestation or conversions
Normalized Difference Soil Index (NDSI) (Lee & Choi, 2023)	Differentiates bare soil using SWIR and NIR

271

272 As presented in Table 1, a range of spectral indices has been widely used in deforestation detection
 273 to evaluate vegetation health, soil exposure, water content, urban expansion, and fire damage based
 274 on satellite-derived spectral bands such as *NIR*, *Red*, and *SWIR*. These indices enhance land-cover
 275 change detection and facilitate the monitoring and quantification of forest degradation over time.

276 5. Analysis of Various Deforestation Change Detection Approaches

277 Figure 8 illustrates the structured classification of deforestation change detection methods divided
278 into traditional, ML, and DL techniques. Each category is further grouped into pixel-based, object-
279 based, and hybrid models, which show the specific algorithms used for accurate forest change
280 analysis.



281

282 Figure 8 Classification of Deforestation Change Detection Techniques Based on Traditional, ML,
283 and DL Approaches.

284 Figure 8 illustrates the structured classification of deforestation change and detection methods divided
285 into traditional techniques, ML, and DL techniques. Each category is further grouped into pixel-
286 based, object-based, and hybrid models, which show the specific algorithms used for accurate forest
287 change analysis. Traditional change detection methods directly compare images whereas pixel-based
288 methods compare pixel values between images. Object-based methods work on groups of pixels
289 instead of a single pixel. Pixel-based ML works on pixel values, object-based ML works on
290 segmented objects, and hybrid ML combines multiple models and does so more accurately than
291 traditional methods. DL models are advanced models that learn automatically. Pixel-based DL
292 operates directly on images to detect patterns. Object-based DL combines deep neural networks with

293 image segmentation to identify, delineate, and classify distinct objects within images rather than just
294 pixels. Hybrid DL models combine multiple deep learning techniques but are highly complex.

295 **5.1 Pixel-Based Approaches**

296 Pixel-based change detection techniques monitor changes at the most basic pixel level, depending on
297 spectral or textural properties from bi-temporal or multi-temporal satellite images. Such methods are
298 based on the analysis of pixel-wise changes, for instance, changes in reflectance values or vegetation
299 indices such as NDVI (Laurance et al., 2014) to make the land-cover transformation visible. These
300 techniques are very simple and less dependent on ground truth data, which gives them a major
301 advantage in uniform forest areas. However, pixel-wise methods can be sensitive to noise,
302 atmospheric conditions, and sensor variations; therefore, they may suffer from reduced accuracy,
303 especially in diverse landscapes. They are computationally inefficient and do not handle the
304 complexities of forest dynamics well. Therefore, machine learning algorithms, such as SVM, RF, and
305 Nearest Neighbour (k-NN) (Torres et al., 2021). DL frameworks have been integrated into pixel-
306 based workflows. Models such as CNNs, U-Nets, Autoencoders, and Siamese networks assist with
307 feature extraction and improve change detection. The main drawback is that the decisions are made
308 for each pixel separately, which may lead to the disregard of important spatial contexts that could
309 have increased accuracy(Wagner et al., 2023)(Dong et al., 2024).

310 **5.2 Object-Based Approaches**

311 Object-based change detection methods segment images into homogeneous objects based on their
312 spatial, spectral, and contextual properties, enabling analysis at the object level rather than the
313 individual pixel level. This approach allows for the extraction of stable and interpretable features that
314 capture the structural patterns associated with deforestation (Laurance et al., 2014) (Pulella et al.,
315 2020). Among the segmentation methods used are Simple Linear Iterative Clustering (SLIC), Simple
316 Non-Iterative Clustering (SNIC), and Superpixels Extracted via Energy-Driven Sampling(SEED),
317 which segment images into meaningful regions (Bergamasco et al., 2022)(Desclée et al., 2013). When

318 object-based methods are combined with machine learning or deep learning algorithms, such as
319 CNNs or decision-tree classifiers, they deliver more precise classification by incorporating spectral
320 and geometric attributes. This is why object-based approaches are well suited for detecting subtle or
321 fragmented changes in forested areas(X. Zhang et al., 2021).

322 **5.3 Hybrid Approaches Combining Pixel and Object Levels**

323 A hybrid change detection method not only enhances accuracy but also takes advantage of the fine-
324 grained sensitivity of pixel-based techniques and the contextual strength of object-based
325 analysis(Selvaraj & Amali D, 2023). The integration of these methods overcomes the shortcomings
326 of each other, such as noise in pixel detection and the ambiguity of the boundaries in object-based
327 detection (Y. Zhang et al., 2024). By integrating spectral, spatial, and temporal features, hybrid
328 models not only improve class separability but also minimise false positives in complex forest areas.
329 The use of SNIC-based segmentation in association with pixel-wise reflectance analysis or object
330 classification enhanced by texture features leads to more dependable outcomes (Richardson et al.,
331 2025). In ML, hybrid techniques, such as Random Forest with rule-based spatial filtering or Support
332 Vector Machines applied to segmented areas, have yielded better accuracy (X. Zhang et al., 2021). In
333 DL, models incorporating Convolutional Neural Networks with long short-term memory or attention
334 modules or those that merge U-Net with object-level post-processing, successfully track both spatial
335 structure and temporal change. These techniques are particularly effective in identifying slight,
336 gradual deforestation trends across various landscapes (Kushwaha, 2025).

337 **5.4. Deforestation Change Detection Based on Traditional, ML, and DL**

338 **5.4.1 Traditional Deforestation Change Detection Methods**

339 As shown in Table 2, conventional deforestation change detection techniques utilise pixel or object
340 based approaches, such as NDVI, PCA, image differencing, and Object-Based Image Analysis
341 (OBIA), to analyse temporal satellite data and identify land-cover transformations.

342 Table 2 Summary of Traditional Change Detection Techniques in Deforestation Monitoring

Approach	Method	Description
Pixel-based	Image Differencing(Arcanjo et al., 2016)	Identifies change by subtracting pixel values from two temporal images, highlighting areas of alteration
	Image Ratioing(Adarme et al., 2020)	Divides pixel values across dates to enhance spectral variation while reducing terrain-related effects.
	PCA (Y. Zhang et al., 2024)	Transforms correlated spectral bands into principal components to detect variance associated with land-cover change.
	NDVI Differencing (Masolele et al., 2021)	Utilises variations in red and NIR reflectance to quantify vegetation loss between image pairs
Pixel-Based or Object-Based	Post Classification Comparison(Chen et al., 2022)	Compares independently classified images to detect changes at the pixel level, useful for discrete land cover shifts
Object-Based	OBIA(Bergamasco et al., 2022)	Segments imagery into homogeneous objects using spectral and spatial characteristics for refined classification
	Rule-Based Object Classification (Reading et al., 2024)	Applies predefined rules on object attributes like shape and texture to assign land cover types

343

344 Traditional change detection methods, such as Image Differencing, NDVI Differencing, and PCA,
345 work by comparing temporal image spectra and analysing pixel-wise spectral variations. In contrast,
346 object-based approaches such as OBIA and Rule-Based Classification rely on spatial features for
347 image segmentation. Many of these techniques struggle with classification due to spectral confusion,
348 shadowing, and pixel mixing in mixed-forest areas. Hence, more robust ML and DL architectures are
349 needed.

350 5.4.2 Machine Learning Models

351 ML models automatically find patterns in data, enabling efficient prediction and classification tasks.
352 Remote sensing is used to map land cover and detect changes in deforestation through the analysis of
353 complex, high-dimensional data, which is performed using supervised, unsupervised, or
354 reinforcement learning strategies, and the performance is improved over time via data-driven training
355 (Durowoju, 2025); (Selvaraj & Amali D, 2023). Table 3 compares different ML methods for

356 deforestation detection, including pixel-, object-, and hybrid models, along with their main findings
 357 and limitations. The models achieved very good classification results however, they had difficulties
 358 due to issues of data quality, spatial resolution, and regional variability.

359 Table 3 Overview of ML Models for Deforestation Change Detection: Key Findings and
 360 Limitations

ML Models	Key Findings	Limitations
Pixel-Based Approach		
RF(Brovelli et al., 2020)(Cazzolla et al., 2025)(L. Gupta et al., 2025)	Efficiently identified forest degradation using satellite imagery	Spatial resolution constraints in some regions.
	Delivered scalable forest loss mapping with minimal tuning.	Struggled with complex transition classes.
	Provided high accuracy for regional forest analysis using NDVI/SAVI.	Misclassified spectrally similar land types.
Maximum Likelihood(Haq et al., 2021)	Highlighted human and climatic drivers of forest cover decline	Limited temporal data restricted full-scale analysis.
RF and Improved Grid Search Optimization (IGSO)(Masolele et al., 2021)	Improved detection accuracy in plantation zones.	Decreased reliability in densely forested zones.
RF(Pacheco-Pascagaza et al., 2022)	Enabled fast change monitoring using Sentinel 2	Geographic limitations affect generalization.
RF and Classification and Regression Tree (CART)(Karishma et al., 2022)	Captured significant land cover transitions due to agriculture.	Historical data gaps limited a comprehensive assessment.
SVM(Potić et al., 2023)	Increased forest classification accuracy.	Insufficient data hindered model performance.
RF, SVM, ANN, KNN, XGBoost (Rash et al., 2023)	Mapped major land use changes due to urbanization	Dataset limitations affected temporal consistency.
SVM, RF, Maximum Likelihood(Atef et al., 2023)	Accurately identified multiple land cover types.	Reduced accuracy in areas with high local variability.
LightGBM(Karmoude et al., 2025)	Achieved fast and efficient classification using vegetation indices.	Poor performance in detecting small-scale deforestation.
SVM and RF(Meiaraj, 2025)	Offered consistent classification across periods.	Performance varies across climatic zones.
SVM (with SNIC)(Selvaraj & Amali, 2023)	Effective object-level forest classification.	Performance is reduced in mixed land types.
PVts-β, RF, NN, SVM, DT, NB (Y. Zhang et al., 2024).	Integrated data sources for tropical forest detection.	The model is limited by geographic and data specificity.
Object-Based Approach		
SVM and k-NN (Selvaraj & Amali D, 2023)	Improved classification using enhanced object features.	Accuracy is impacted by input quality.
Hybrid Approach		
ML and Rule-based hybrid(Reading et al., 2024)	Enabled near-real-time alerts for deforestation.	Manual verification needed; lacks full automation.

RF, SVM, DT, XGBoost, MLP, U-Net, LSTM (Richardson et al., 2025)	Combined ML and DL for accurate deforestation trend mapping.	Demands extensive training and harmonized inputs.
--	--	---

361

362 ML studies show that RF, SVM, and Maximum Likelihood classifiers have been effective in mapping
363 deforestation using NDVI, spectral, and object-level inputs. However, these methods often cannot
364 cope with complex forest structures and spectrally similar areas. The models are feature-based, which
365 makes them dependent on the quality of the input data, climate variations, and timing inconsistencies.
366 Light GBM is fast but lacks the precision of XGBoost at fine scales. The increase in data nonlinearity
367 and the region-specific nature of forest dynamics lead ML models to perform poorly. Thus, deep
368 learning and hybrid models that provide scalable, contextually learned, and adaptable capabilities
369 across different landscapes for accurate deforestation monitoring are needed.

370 5.4.3 Deep Learning Models

371 Deep learning relies heavily on hierarchical neural networks and is characterised by accurate feature
372 extraction, land cover classification, and change detection. The deep learning models applied to
373 deforestation change detection are listed in Table 4, along with their major contributions to accuracy
374 and automation. Yet, issues such as limited data, high computational costs, and regional generalization
375 affect the performance of even complex DL models.

376 Table 4 Summary of Deep Learning Approaches for Deforestation Change Detection

DL Model	Key Findings	Limitations
Pixel-Based Approach		
Early Fusion, Siamese Network, Convolution SVM (Adarme et al., 2020)	Achieved improved detection accuracy with reduced noise in forest change analysis.	Requires evaluation of alternative architectures to lower false alarms.
Cycle Generative Adversarial Network (GAN)(Soto Vega et al., 2021)	Enabled deforestation detection without labelled data using image translation.	Accuracy varies across tropical biome types.
Variational Autoencoder (VAE)(Zerrouki et al., 2021)	Demonstrated efficient detection of land degradation patterns.	Region-specific application due to limited satellite sources.
Orthogonal Unsupervised Discriminant Projection(OU DP), Radial-Basis Function (RBF)	Unsupervised learning effectively highlighted forest changes.	Clustering output depends on sensitive parameter settings.

Based Clustering.(N. Gupta et al., 2021)		
U-Net, ResU-Net, SegNet, FC-DenseNet, DeepLabv3+(Torres et al., 2021)	CNNs accurately captured deforestation in optical imagery.	Limited data caused reduced model generalization.
CNN, GNN, Transformer(Y. Zhang et al., 2024)	Attention-based methods enhanced forest change mapping	Inconsistent outcomes across varied image sources.
DeepLabv3+ semantic segmentation(de Andrade et al., 2022)	Semantic segmentation improved deforestation detection in tropical forests.	Training demands high computational resources.
U-Net(Masolele et al., 2022)	Accurately classified deforestation patterns using vegetation metrics.	Restricted by limited temporal and spatial coverage.
Attention U-Net(John & Zhang, 2022)	Model adapted well to image-specific deforestation detection.	Performance varied with satellite data types.
DeepLabv3+ and Deeply Supervised Image Fusion Network (Javed et al., 2023)	Detected urban forest changes using fused imagery.	Temporal gaps and regional bias reduced accuracy.
RRCNN-1, RRCNN-2 and RRCNN-3(Neves et al., 2023)	Applied residual and recurrent learning for SAR-based monitoring.	Constrained to limited SAR datasets.
SiamHRnet-OCR(Wang et al., 2023)	Delivered high accuracy in high-resolution forest monitoring.	Dependent on satellite availability and image quality.
Unsupervised Progressive Learning Framework (UPLF).(Y. Zhou et al., 2023)	Progressive learning supported unsupervised change analysis.	Performance fluctuated under image variability.
Domain Adversarial Neural Network (DANN)(Vega et al., 2023)	Detected forest changes using weak supervision effectively.	Dataset imbalance affected generalization.
U-Net(Wagner et al., 2023)	Demonstrated reliable forest loss detection.	Limitations in long-term monitoring due to coarse time resolution.
U-Net with EfficientNet-B3(Fodor & Conde, 2023)	Identified burned and deforested regions with high precision.	Remote area data scarcity impacted reliability.
R2U-Net, Attention U-Net, Attention R2U-Net and Nested U-Net(Lee & Choi, 2023)	Leveraged diverse inputs for comprehensive mapping.	Change detection reduced by limited revisit frequency.
DL-DEGRAD(Dalagnol, Wagner, et al., 2023)	Captured tropical degradation patterns via learned features.	Failed to detect subtle changes in coarse imagery.
Self-supervised Contrastive Learning Transformer (SWCL-T)(Dong et al., 2024)	Performed unsupervised change analysis robustly on SAR images.	High complexity and SAR-only support limited applicability.
Swin Transformer V2, VGG16, Mixed Feature Pyramid (MFP)(Zheng et al., 2024)	Combined multiscale features for accurate binary detection.	Dual-branch model increased resource requirements.
Transformer-based model using an attention mechanism(Alshehri et al., 2024)	Achieved state-of-the-art accuracy using bi-temporal imagery.	Computational cost and low interpretability are concerns.
U-Net (customized with 13 tensor inputs)(Moni et al., 2025)	Enabled long-term multi-class mapping with the Landsat series.	Misclassification issues due to striping and index variations.
Hybrid Approach		

DL with Multinomial Logistic Regression + Softmax(Srivastava & Ahmed, 2024)	Mapped transitions effectively using learned pixel relationships.	Relies on prior classification; lacks end-to-end learning.
CNN Ensemble (AlexNet to Swin)(Coşolan & Moldovan, 2024)	Successfully transferred features across forest types.	Accuracy is reduced across ecosystems, and ensemble complexity is high.
Modified U-Net in Siamese structure and Feature Aggregation Module(X. Li et al., 2025)	Introduced generative consistency for accurate binary detection.	Relies on controlled noise, moderately compute-intensive
Convolutional Wavelet Neural Network (CWNN), Deep Convolutional Generative Adversarial Network (DCGAN) (X. Zhang et al., 2021)	Accurately detected localized forest change using wavelet-texture fusion.	Model generalizability is tested in varied environments.
DeepForest-1a/b/c, DeepForest-2a/b (Cherif et al., 2022)	Provided land use classification using combined SAR and optical inputs.	Limited training data influenced regional performance.
Transformer-based Multiscale Siamese Framework (TMSF) (Tarazona et al., 2021)	Achieved accurate results by fusing local-global representations.	Boundary clarity and semantic context remain limitations.
U-Net and ResNet-34(pre-trained) (Kushwaha, 2025)	Improved forest segmentation using residual learning on aerial imagery.	Limited to single-date images and mask quality.

377

378 According to DL case studies, U-Net, Res U-Net, and DeepLabv3+ have demonstrated superior
379 performances in semantic segmentation and vegetation detection. Transformers and Siamese
380 networks enhance spatiotemporal awareness using attention mechanisms. GANs facilitate the
381 utilization of unlabelled data, whereas VAE, CCWNN, and contrastive learning provide robust
382 capabilities for pattern extraction. However, several challenges remain, such as reliance on high-
383 quality satellite imagery, computational demands of these models, and limited temporal
384 generalization. Despite these obstacles, deep learning surpasses traditional machine learning in terms
385 of scalability, contextual adaptability, and feature autonomy. As forest dynamics become increasingly
386 nonlinear and data-rich, the development of advanced hybrid models that integrate multimodal inputs
387 and cross-domain learning is crucial for accurate, generalised mapping of deforestation across diverse
388 environments.

389 Deforestation change detection has evolved from spectral and index-based techniques to spatial-
390 temporal and multimodal frameworks because early methods were often sensitive to heterogeneous

391 landscapes, spectral confusion, and seasonal variability. As monitoring tasks became more complex,
 392 object-based, hybrid, and deep learning approaches gained importance because they could better
 393 capture contextual, multiscale, and temporal change patterns. More recently, Transformer based
 394 models have attracted attention for their ability to model long range spatial relationships, although
 395 their computational demands remain high. Despite these advances, persistent challenges include
 396 limited cross regional generalisation, domain shift across sensors and acquisition conditions,
 397 annotation scarcity, and class imbalance in deforestation datasets.

398 5.5 Benchmark Datasets for Deforestation Change Detection

399 To enable reproducibility and standardised evaluation, deforestation change detection based on
 400 satellite imagery has used the most widely recognised benchmark datasets. These datasets have
 401 varying spatial resolutions, temporal intervals, geographic extents, and sensor modalities, enabling
 402 rigorous cross-model assessments and increasing the reliability and generalizability of deep learning
 403 methodologies in remote sensing. The most widely used datasets for deforestation change detection
 404 are provided in Table 5, which includes high-resolution optical and SAR-based sources for monitoring
 405 forest loss. These datasets enable applications such as trend analysis, real-time alerts, and training
 406 deep learning models across diverse regions.

407 Table 5 Commonly Used Datasets for Deforestation Change Detection

Dataset Name	Source	Description
LEVIR-CD (Zheng et al., 2024),(X. Li et al., 2025), (Tarazona et al., 2021)	WHU, China	High-resolution RGB image pairs (1024×1024) annotated for urban change and also used in forest boundary detection.
WHU-CD (Zheng et al., 2024),(X. Li et al., 2025),(Tarazona et al., 2021)	Wuhan University	Annotated building footprint changes, often adapted for deforestation in high-resolution imagery.
SYSU-CD (Zheng et al., 2024),(X. Li et al., 2025),	Sun Yat-Sen University	RGB images designed for general change detection; applied in forest cover mapping.
CDD (Tarazona et al., 2021)	Cloud-CD Dataset	Bi-temporal optical imagery designed to evaluate robustness in cloud-prone scenes.
Planet Amazon NICFI (Dalagnol, Wagner, et al., 2023), (Richardson et al., 2025)	Planet Labs	High-resolution monthly monitoring data used for tracking tropical deforestation.
Hansen Forest (Adarme et al., 2020)	Global Forest Watch	Global annual forest cover loss with pixel-level labels; used in trend forecasting.

Global Forest Change (GFC)(M. C. Hansen et al., 2013)	University of Maryland,	Global maps of forest cover, gain, and annual forest loss derived from Landsat imagery.
PRODES (Wagner et al., 2023)	INPE, Brazil	Annual deforestation mapping in the Legal Amazon with validated polygons.
RADD Alerts (Masolele et al., 2021)	Global Forest Watch / Wageningen University	Real-time alerts for tropical forest loss based on Sentinel-1 SAR imagery.

408

409 Beyond their availability, these benchmarks differ in the type of evidence they provide for model
410 design and evaluation. LEVIR-CD, WHU-CD, SYSU-CD, and CDD are primarily high-resolution
411 remote-sensing change-detection benchmarks and are more suitable for testing fine-scale change
412 boundaries and binary segmentation architectures than for direct ecological generalisation in
413 deforestation studies(Cheng et al., 2024) . Hansen Global Forest Change (GFC) is more appropriate
414 for pixel-level regional or global forest-loss analysis, while PRODES is especially valuable when
415 official annual deforestation mapping is needed for area-based assessment (Wu et al., 2025)(Beyer et
416 al., 2025)(Messias et al., 2024). Planet NICFI is particularly useful for monitoring small clearings
417 because of its 5 m spatial detail and monthly tropical coverage, whereas RADD alerts are more
418 appropriate for near-real-time monitoring in persistently cloudy humid tropics because they rely on
419 cloud-penetrating Sentinel-1 radar(Wagner et al., 2023)(Doblas et al., 2022)(Welsink et al., 2023).
420 Taken together, the current benchmark landscape is still stronger for binary change detection than for
421 standardised multiclass change mapping; this is best treated as an inference from recent benchmark
422 reviews, which also show that transferability depends strongly on sensor type, annotation design, and
423 geographic context (Beyer et al., 2025)(Cheng et al., 2024).

424 **5.6 Comprehensive Comparison and Applicability Analysis**

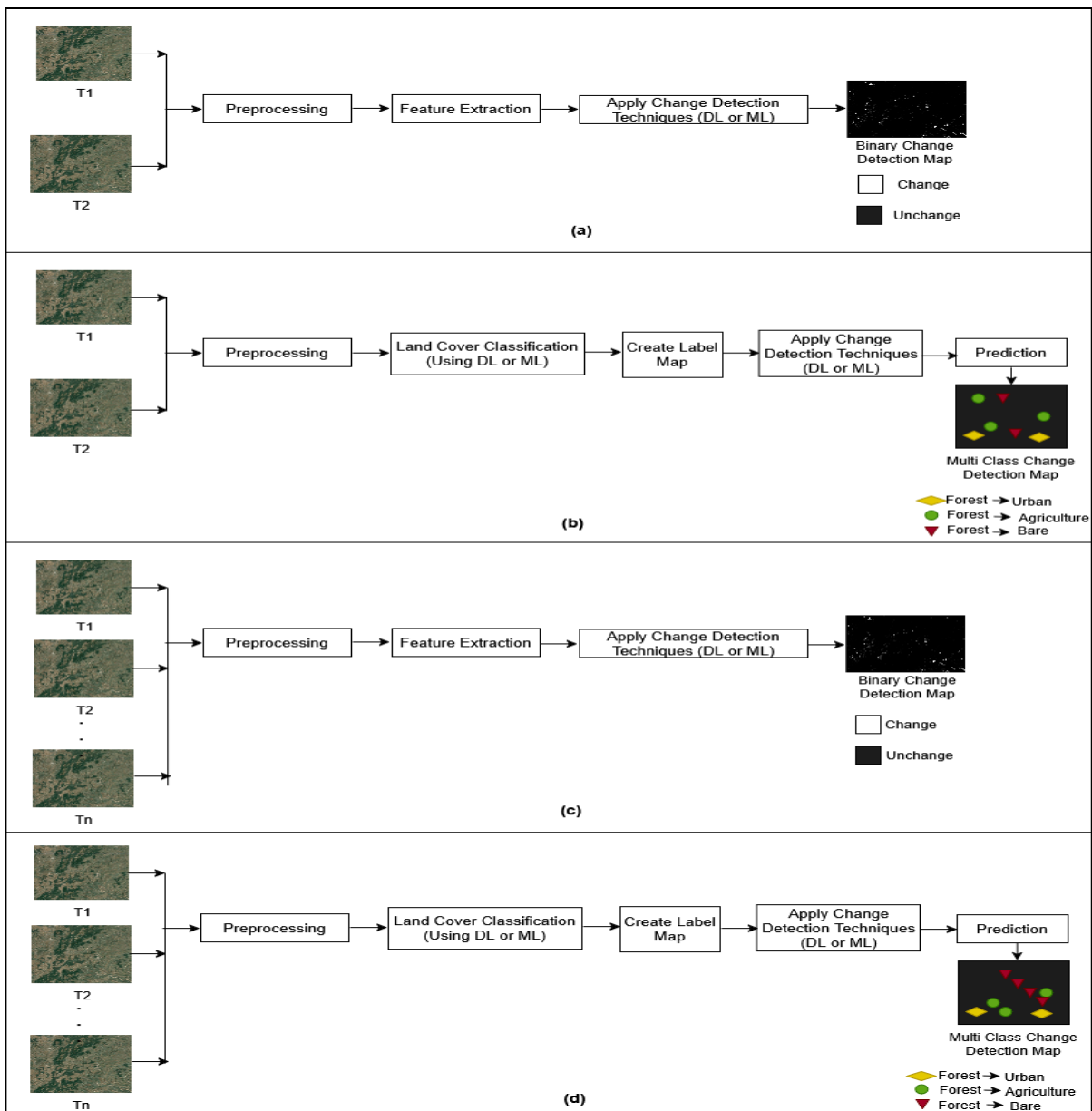
425 Pixel-based and traditional methods work well for spectrally clear-homogeneous data, but they
426 underperform when there is spectral confusion. Classic classifiers such as Maximum Likelihood and
427 CART are less commonly used than RF and LightGBM in medium-resolution applications (Karmoude
428 et al., 2025). ML models are more suitable for resource limited and large-scale operational monitoring.
429 On the other hand, DL models perform better in heterogeneous and complex forest environments with

430 high spatial variability. Although they require greater resources, DL models are still widely used
431 because they offer good segmentation performance at a manageable computational cost. But
432 transformer-based models require more memory with longer training time. They also usually require
433 more data, especially for tasks like optical–SAR fusion and temporal modelling. The performance of
434 advanced DL models is often limited by labelled data scarcity and cross regional generalization issues
435 (Zheng et al., 2024)(Alshehri et al., 2024). Multimodal and hybrid DL frameworks improve contextual
436 learning but increase implementation complexity. So, the choice of the algorithm should not only
437 depend on the performance but also on the availability of the data and computing resources.

438 **6. Deforestation Change Detection Based on Output Map**

439 Change detection outputs in deforestation monitoring primarily fall under two categories: binary and
440 multi-class. Figure 10 illustrates the workflows for binary and multi-class deforestation change
441 detection using bi-temporal and multi-temporal satellite image data. It compares direct feature-based
442 approaches with land-cover classification methods that employ ML or DL techniques to generate
443 change maps.

444



445

446 **Figure 9** Workflow Architectures for Binary and Multi-class Deforestation Change Detection Using
 447 DL and ML Techniques (a) Binary Change Detection Map Using Bi-Temporal Imagery, (b) Multi-
 448 class Change Detection Map Using Bi-Temporal Imagery Binary Change Detection, (c) Binary
 449 Change Detection Map Derived from Multi-temporal Imagery, (d) Multi-class Change Detection Map
 450 Derived from Multi-temporal Imagery

451 Figure 9 illustrates four change detection strategies based on temporal input and output type.
 452 Comparison of bi-temporal imagery helps detect if a change has occurred or not, with multi-class
 453 change detection using bi-temporal imagery we can identify the land type and then determine if
 454 change has occurred or not. With multi-temporal imagery from different years, a model can find if

455 any change has happened over time or can identify different land types, then determine what type of
456 changes happened over the years.

457 **(a) Binary Change Detection Map Using Bi-Temporal Imagery**

458 Binary change detection using bi-temporal satellite imagery is extensively utilised in
459 deforestation monitoring because of its efficiency in generating "change/no-change" outputs.
460 Models such as hybrid RF-NDVI (Reading et al., 2024) and LightGBM with vegetation indices
461 (Karmoude et al., 2025) offers rapid and resource-efficient mapping. Advanced approaches,
462 such as UPLF (Y. Zhou et al., 2023), Siamese CNNs (Adarme et al., 2020), (X. Li et al., 2025)],
463 and transformer-based models (Alshehri et al., 2024), provide accurate segmentation without
464 requiring extensive annotations. Recent innovations include SiamHRnet-OCR for high-
465 resolution binary mapping, DeepLabv3+ for handling data imbalance (Javed et al., 2023), and
466 domain-adaptive methods using GANs (Soto-Vega et al., 2021). Collectively, these methods
467 ensure scalable and precise forest-loss detection for large-scale environmental monitoring
468 systems.

469 **(b) Multi-class Change Detection Map Using Bi-Temporal Imagery**

470 The application of multi-classification to bi-temporal data has improved the analysis of
471 deforestation, shifting from simple binary classifications to the detection of land-use changes
472 across diverse categories. Some studies, such as those of Karishma et al. (Karishma et al.,
473 2022) and (Karishma et al., 2022) found that scalable multi-class outputs were possible by
474 using spectral data and NDVI-derived inputs (Cazzolla et al., 2025). Although they are very
475 complex, deep learning algorithms such as DeepLabv3+ (Javed et al., 2023) and DL-DEGRAD
476 techniques have successfully detected various types of degradation in Planet NICFI data.
477 Moreover, the combination of Sentinel data and global bi-temporal datasets has consolidated
478 mapping capabilities in areas with frequent cloud cover.

479

480 **(c) Binary Change Detection Map Derived from Multi-temporal Imagery**

481 Multitemporal satellite imagery is a significant advantage for binary change detection because
482 it captures gradual deforestation patterns and minimises seasonal misclassifications. The
483 applied combined technology of both ML and DL models, such as RF, U-Net, and LSTM on
484 Landsat time series (Richardson et al., 2025) and Random Forest in GEE using NDVI/SAVI
485 indices (L. Gupta et al., 2025) increased the temporal consistency of the studies. One of the
486 variants of U-Net (Wagner et al., 2023), (Lee & Choi, 2023), and transfer learning using CNNs
487 (Coşolan & Moldovan, 2024) achieved high accuracy. U-Net models on the Sentinel-2 and
488 Planet NICFI datasets (Dalagnol, Wagner, et al., 2023), (Richardson et al., 2025) effectively
489 monitored deforestation in Ukraine and Brazil. Additionally, the RRCNN series (Neves et al.,
490 2023) and comparative analysis with PRODES (Wagner et al., 2023) enabled consistent
491 detection of subtle and large-scale forest changes.

492 **(d) Multi-class Change Detection Map Derived from Multi-temporal Imagery**

493 The use of multiclass classification with multi-temporal images has provided a robust
494 description of land-use changes and ecological shifts, thereby facilitating more strategic forest
495 management. Different methods, such as the supervised classification of optical data (Haq et
496 al., 2021) and ensemble ML models (Rash et al., 2023), have successfully revealed the effects
497 of human activities on the environment. The application of sequential spectral inputs is an
498 important factor in long-term mapping (Richardson et al., 2025), (Meiaraj, 2025). Among
499 others, DL-DEGRAD (Dalagnol, Wagner, et al., 2023), modified U-Net (Moni et al., 2025),
500 and DLCD (Srivastava & Ahmed, 2024) These are deep learning models that can detect a wide
501 range of transitions. Other strong methods, such as DeepForest and CNN-based predictors that
502 operate on multi-sensor time series, have enabled dynamic multi-class labelling. Although

503 these models require substantial computational resources, they still play an important role in
504 domains such as REDD+, carbon tracking, and land-use forecasting across diverse landscapes.

505 7. Result and Discussion

506 This section presents a detailed comparison of ML and DL models for detecting deforestation
507 changes, accompanied by visual aids and performance tables. The analysis revolved around
508 factors such as the data source, Task category, algorithmic strategies, analysis levels, and output
509 classifications.

510 7.1 Common Performance Metrics

511 Evaluation metrics are essential for assessing the effectiveness of deforestation change
512 detection models by measuring classification accuracy, error rates, and spatiotemporal
513 reliability using indicators such as precision, recall, F1-score, overall accuracy, kappa,
514 Intersection over Union (IoU), and user/producer accuracy. High OA might still be observed in
515 deforestation mapping despite missing many deforested pixels because the non-deforested
516 class usually covers most of the image. F1-score is preferable than OA as it combines both
517 precision and recall (Z. Zhou et al., 2023). IoU is also more useful because it directly measures
518 the overlap between the predicted deforested area and the reference area. (Farhadpour et al.,
519 2024). Maxwell et al. showed that reporting only OA can be misleading in the presence of class
520 imbalance, especially when the background class is dominant(Maxwell & Warner, 2026).
521 Therefore, for rare-class problems such as deforestation detection, F1-score and IoU give a
522 more realistic view of model reliability than OA alone.

$$P = \frac{TP}{TP + FP} \quad (12)$$

$$R = \frac{TP}{TP + FN} \quad (13)$$

$$F1 = 2 \times \frac{Precision \cdot Recall}{Precision + Recall} \quad (14)$$

$$OA = \frac{TP + TN}{TP + TN + FP + FN} \quad (15)$$

$$K = \frac{P_o - P_e}{1 - P_e} \quad (16)$$

$$IoU = \frac{TP}{TP + FP + FN} \quad (17)$$

$$AA = \frac{TP + TN}{P + N} \times 100 \quad (18)$$

523 Precision (P), Recall (R), F1-Score (F1), Overall Accuracy (OA), User's Accuracy (UA),
 524 Producer's Accuracy (PA), Alarm Area (AA), TP-True Positive, TN-True Negative, FP-False
 525 Positive, FN-False Negative, Table 7 enumerates the prominent evaluation metrics used to
 526 assess deforestation change detection models, namely precision, recall, F1-score, overall
 527 accuracy, IoU, kappa, and user/producer accuracy.

528 7.2 Evaluation of ML-Based Models

529 Table 6 presents a comparison of the performance of different ML models for deforestation
 530 change detection, indicating that these models achieve high overall accuracy and kappa, with
 531 the LightGBM- and SVM-based approaches leading. The ML models have shown excellent
 532 accuracy, especially in pixel-based implementations such as RF, SVM, and LightGBM. In
 533 particular, LightGBM (Karmoude et al., 2025) achieved the highest overall accuracy (99.3%)
 534 and Kappa coefficient (0.986) using Sentinel-2 bi-temporal imagery, which was enhanced with
 535 vegetation indices. Similarly, hybrid methods that combine U-Net, RF, and LSTM (Richardson
 536 et al., 2025) also yielded a 99% OA. Classic models such as Maximum Likelihood (Haq et al.,
 537 2021) and optimised RF (Masolele et al., 2021) were at par in terms of accuracy, scoring
 538 between 93% and 96%.

539

540

541 **Table 6** Comparison of ML models for deforestation monitoring grouped by classification
 542 type and task category.

Category	Reference	ML Model	OA (%)	K(%)	P(%)	R(%)
Binary Classification						
Forest change/deforestation / forest-loss detection	(Brovelli et al., 2020)	RF	0.95	0.91	0.98	0.93
	(Cazzolla et al., 2025)		80	-	-	-
	(L. Gupta et al., 2025)		88.76	0.87	91.95	-
	(Karmoude et al., 2025)	LightGBM	84.8	0.73	0.65	-
Forest/vegetation detection and monitoring	(Potic et al., 2023)	SVM	99.01	-	-	-
Near real time deforestation alter	(Oca et al., 2025)	ML and Rule-based hybrid	91.84	-	-	-
Multiclass Classification						
Forest cover / land-cover classification and change detection	(Haq et al., 2021)	Maximum Likelihood	94.6	0.93	-	-
	(Karishma et al., 2022)	RF and Classification and Regression Tree (CART)	85	-	-	-
	(Rash et al., 2023)	XGBoost	96.67	0.96	-	-
	(Atef et al., 2023)	SVM, RF, Maximum Likelihood	95.95	0.94	-	-
	(Selvaraj & Amali, 2023)	SVM (with SNIC)	94.42	0.9207	-	-
	(Selvaraj & Amali D, 2023)	SVM and k-NN	0.92	-	-	-
	(Meiaraj, 2025)	SVM and RF	0.94	0.92	-	-
Plantation / crop-related classification	(K. Xu et al., 2021)	Improved Grid Search optimisation (IGSO)	96.08	0.94	-	-
Near-real-time vegetation / forest-loss monitoring	(Pacheco-Pascagaza et al., 2022)	RF	92.5	-	-	-
Tropical deforestation detection	(Tarazona et al., 2021)	PVts- β , RF, NN, SVM, DT, NB	95.09	93.18	-	-

543

544 **7.3 Evaluation of DL-Based Models**

545 The performance of deep learning models for detecting deforestation changes is illustrated in

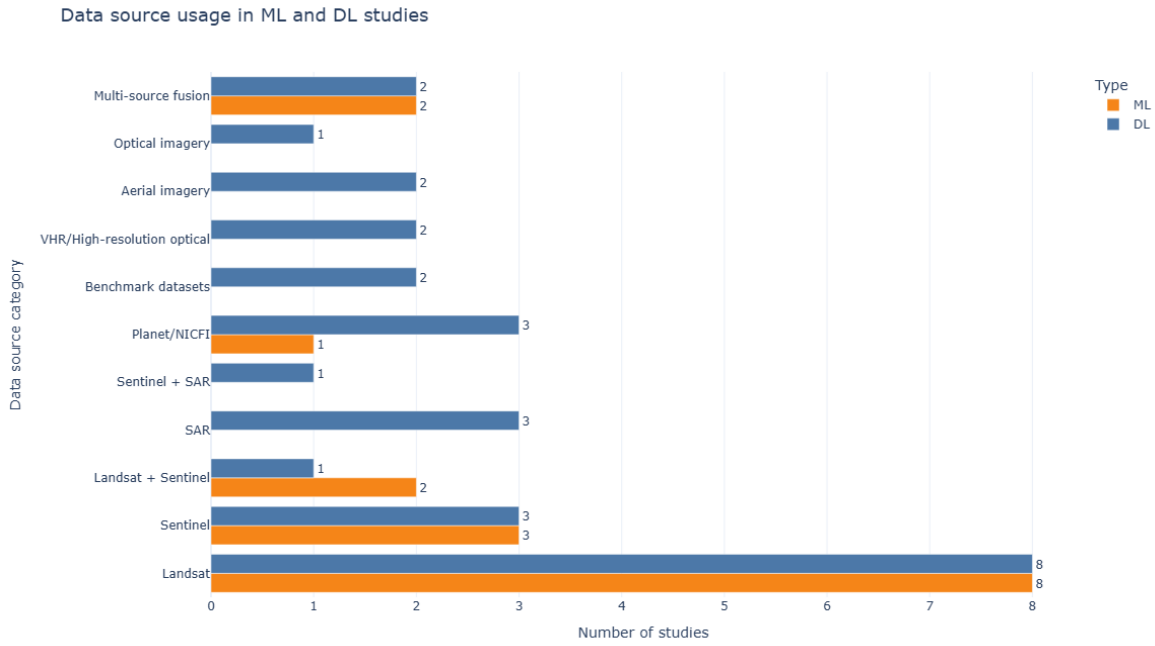
546 Table 7, with high accuracy and F1-scores already achieved by U-Net variants, Transformers,

547 and GANs, indicating great potential for reliable forest monitoring. The deep learning models
548 had the best classification power among all tasks, regardless of whether they were binary or
549 multi-class. CNN-based architectures achieved 99.7% OA and 99.1% precision (Torres et al.,
550 2021). In contrast, transformer-based frameworks, such as SWCL-T (Dong et al., 2024) and
551 Swin Transformer V2 (Zheng et al., 2024), performed very well throughout, with F1-scores of
552 nearly 0.92. TMSF (Tarazona et al., 2021), a hybrid model that fuses multi-scale and attention
553 mechanisms, was the one that produced the most consistent outcomes (F1 > 95%, IOU > 90%).

554 **Table 7** Comparison of DL models for deforestation monitoring grouped by classification
555 type and task category.

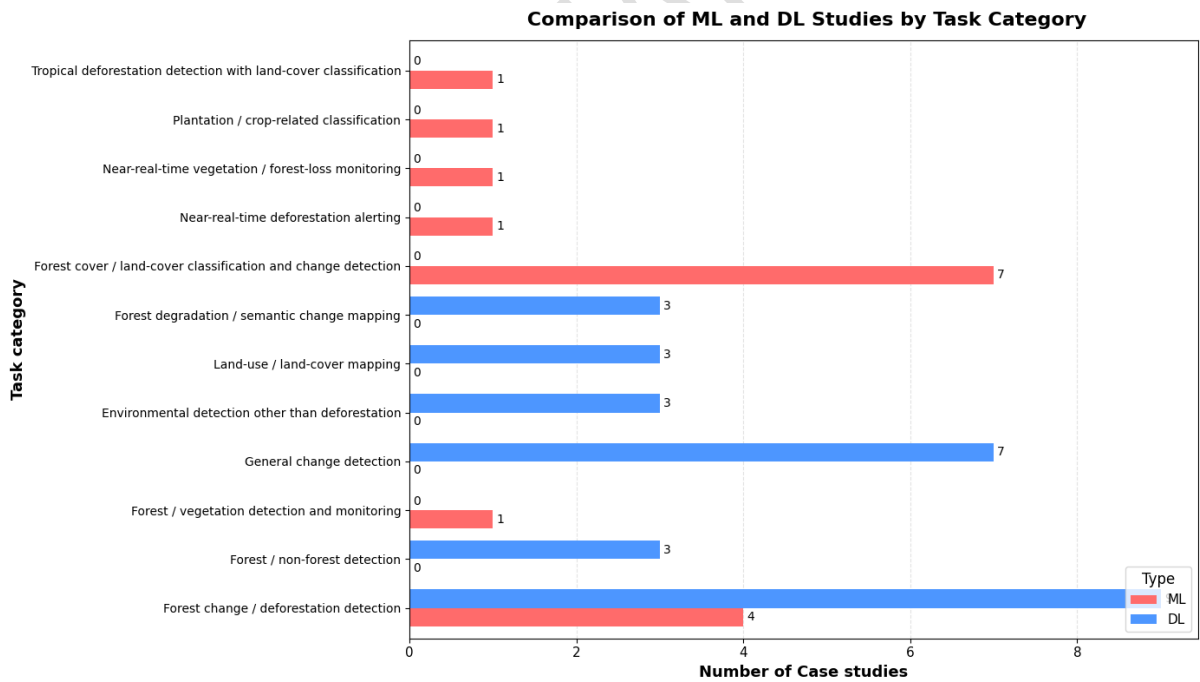
Category	Reference	DL Model	OA (%)	F1	P (%)	R (%)	IoU (%)	K (%)
Binary Classification								
Deforestation/ Forest Change Detection	(Adarme et al., 2020)	Early Fusion, Siamese Network, Convolution SVM	98.0	63.2	-	-	-	-
	(Soto Vega et al., 2021)	CycleGAN	-	85.5	-	-	-	-
	(Torres et al., 2021)	U-Net, ResU-Net, SegNet, FC-DenseNet, DeepLabv3+	-	78.0	-	-	-	-
	(de Andrade et al., 2022)	DeepLabv3+ Semantic Segmentation	-	73.42	-	-	-	-
	(Neves et al., 2023)	RRCNN-1, RRCNN-2, RRCNN-3	-	71.6	97.4	56.7	-	-
	(Wang et al., 2023)	SiamHRnet-OCR	98.98	68.92	64.82	78.97	-	-
	(Vega et al., 2023)	Domain Adversarial Neural Network (DANN)	-	81.6	-	-	-	-
	(Lee & Choi, 2023)	R2U-Net, Attention U-Net, Nested U-Net	-	90.0	-	-	-	-
	(Alshehri et al., 2024)	Transformer (Attention-based)	93	90	84.70	84.53	-	-
Forest / Non-forest segmentation with deforestation implications	(John & Zhang, 2022)	Attention U-Net	-	97.0	-	-	-	-
	(Wagner et al., 2023)	U-Net	98.11	98.0	98.0	-	-	-
	(Kushwaha, 2025)	U-Net	87.0	-	-	-	78.0	-

General change detection	(X. Zhang et al., 2021)	CWNN, DCGAN	99.61	-	-	-	-	-
	(N. Gupta et al., 2021)	OUDP, RBF Clustering	95.77	-	-	-	-	-
	(Y. Zhang et al., 2024)	CGMMA	99.32	92.81	-	-	86.58	-
	(Y. Zhou et al., 2023)	UPLF	-	95.43	94.05	96.86	-	-
	(Dong et al., 2024)	Self-supervised Weighted Contrastive Learning with Transformer (SWCL-T)	98.42	-	-	-	-	93.96
	(Zheng et al., 2024)	Swin Transformer V2, VGG16, CBAM, SSL, and Mixed Feature Pyramid (MFP)	99.79	99.15	99.18	99.13	99.12	94.02
	(X. Li et al., 2025)	U-Net in Siamese	-	92.66	93.53	91.8	86.34	-
Environmental detection other than deforestation	(Zerrouki et al., 2021)	Variation Autoencoder (VAE)	98.0	98.0	-	-	-	-
	(Fodor & Conde, 2023)	U-Net	90.7	88.0	-	-	80.0	-
	(Coşolan & Moldovan, 2024)	VGG19	-	92.0	93.0	91.0	-	-
Multiclass Classification								
Land-use / Land-cover and post-deforestation mapping	(Cherif et al., 2022)	DeepForest-1a/b/c, DeepForest-2a/b	77.9	92.0	-	-	-	-
	(Masolele et al., 2022)	U-Net	-	79.0	-	-	-	-
	(Moni et al., 2025)	Customized U-Net (13 Tensor Inputs)	84.0	81.0	82.0	79.0	68.0	-
Forest degradation / Semantic change mapping	(Javed et al., 2023)	DeepLabv3+ and Fusion Network	-	91.5	-	-	84.4	88.7
	(Dalagnol, Wagner, et al., 2023)	DL-DEGRAD	99.36	84.0	80.0	88.0	-	-
	(Srivastava & Ahmed, 2024)	DL with Multinomial Logistic Regression and softmax	91.80	-	-	-	-	-



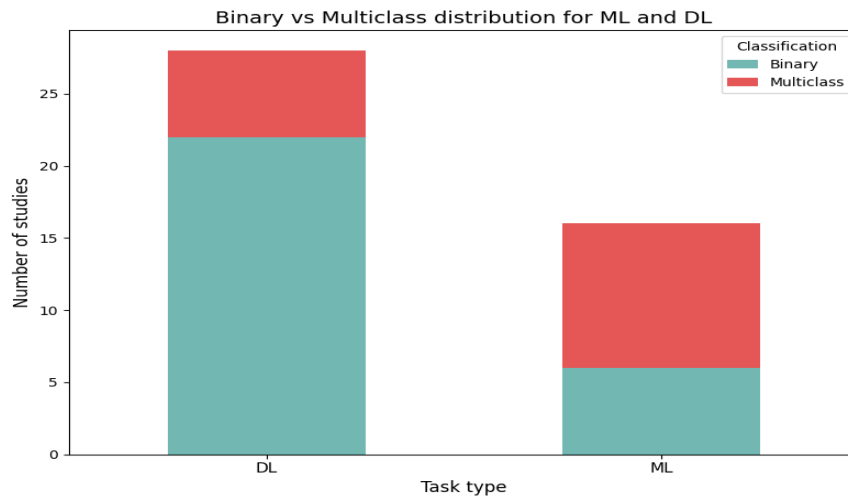
557

558 **Figure 10** Distribution of data-source categories used in ML and DL studies for deforestation
 559 monitoring.



560

561 **Figure 11.** Comparison of ML and DL case studies across task categories for deforestation
 562 monitoring



563

564 **Figure 12.** Binary and multiclass distribution of ML and DL studies for deforestation
 565 monitoring.

566 Figure 10 shows that both ML and DL studies are mainly focused on Landsat and Sentinel data,
 567 which remain the most widely used sources for deforestation-related analysis. Figure 11 depicts
 568 the task category comparison, which suggests that DL approaches are more commonly applied
 569 to forest change detection, forest/non-forest mapping, general change detection, and semantic
 570 change analysis. Figure 12 compares binary and multiclass study distributions for ML and DL,
 571 showing that DL is used much more often in binary classification tasks. ML studies are fewer
 572 overall and show a more balanced distribution, with multiclass studies slightly exceeding
 573 binary ones.

574 7.3. Socio-Environmental Implications and Corporate Accountability

575 Satellite-based monitoring developed under the REDD+ Measurement, Reporting, and
 576 Verification (MRV) system allows independent tracking of forest cover, degradation, and
 577 carbon stocks. This helps to compare the actual environmental changes with corporate
 578 sustainability claims thereby uncover greenwashing. At the same time, remote sensing data can
 579 reveal deforestation hotspots, leakage effects, and ecosystem degradation linked to commodity
 580 production, allowing the identification of climate-related physical risks across global supply
 581 chains (Brovelli et al., 2020). In addition, deforestation-driven land-use changes contribute to

582 regional air and water pollution, which can be effectively monitored by analysing satellite
583 environmental data. Furthermore, integrating analytical methods such as PCA, Epidemic
584 Keratoconjunctivitis(EKC), and the Tapio model helps understand linkages in pollution growth
585 and supports green innovation and sustainable policy decisions(Ma, S. 2025) (Ma et al., 2026).
586 Environmental, Social, and Governance (ESG) is a framework used to measure a company's
587 impact on the planet and people. High-resolution monitoring data can improve ESG rating
588 consistency by providing a common and transparent 'truth layer' for all rating agencies. This
589 reduces the reliance on subjective assessments and ensures consistent, real-world
590 environmental performance (Yan et al., 2025). In this study, data on 133 Chinese A-share
591 companies from 2010 to 2022 were analysed using the Data Envelopment Analysis (DEA)
592 model to measure green innovation performance, and a fixed-effects regression model was used
593 to analyse the impact of ESG on innovation. ESG disclosure by companies improve green
594 innovation and will help perform better on environmental metrics. It also makes companies
595 transparent and trustworthy.(C. Xu et al., 2025). The authors conducted the study on A-share
596 listed companies from 2008 to 2023. They discuss how network effects or spillovers arise when
597 companies influence each other, especially in supply chains. When it comes to climate risk
598 external pressure and internal thinking affect companies. Due to external pressure, suppliers
599 cannot hide information and find it hard to engage in greenwashing whereas due to internal
600 thinking the companies avoid false environmental claims. The other important factors include
601 power, technology and resources, which increase the supply chain pressure. These factors along
602 with laws drive companies to improve their environmental behaviour (Zhong, Yan, et al., 2026).
603 Advanced DL models enhance transparency by analysing ESG and environmental data to
604 identify inconsistencies in corporate sustainability claims. This empowers retail investors to
605 detect greenwashing and take informed actions, thereby promoting greater corporate
606 accountability and more ethical behaviour (Liu et al., 2024)

607 **8. Challenges and Future Directions**

608 Despite significant advancements, deforestation change detection using ML and DL models
609 faces persistent limitations. Data dependency and label scarcity remain critical, with weakly
610 supervised models (Y. Zhou et al., 2023)(Vega et al., 2023) often underperforming in complex
611 ecosystems. Temporal and spatial variabilities affect generalisation (Neves et al., 2023). High-
612 performing architectures, such as the Swin Transformer (Zheng et al., 2024) and Siamese
613 networks (X. Li et al., 2025), require extensive computational resources, which limit their real-
614 time applications. Moreover, noise and spectral confusion in optical imagery (Alshehri et al.,
615 2024)(Moni et al., 2025)(L. Gupta et al., 2025) degrade the classification accuracy. Multiclass
616 classification remains challenging because of class imbalance and overlapping land cover
617 (Srivastava & Ahmed, 2024), (Masolele et al., 2022). In addition, the limited integration of
618 object-based methods (Selvaraj & Amali, 2023) restricts their spatial interpretability. Future
619 research must focus on scalable, label-efficient models, cross-regional adaptability robust
620 preprocessing to counter atmospheric interference, and enhanced fusion of spatial hierarchies
621 to support interpretable, high-resolution outputs.

622 Another research direction can consider the balance between fast detection and reliable forensic
623 results. While some require quick alert systems for timely action, other tasks such as
624 compliance reporting and environmental lawsuits require more accurate results. (Zeng et al.,
625 2025). Thus, multi-stage AI monitoring systems that combine fast screening with accurate
626 results are valuable. Use of AI-based digital tools will improve environmental governance.
627 With these improvements, remote sensing can not only detect forest loss but also promote
628 transparency, accountability, and sustainable development(Ma et al., 2026).

629 **8.1 Emerging Technologies for Next-Generation Forest Monitoring:**

630 New technologies will reshape forest monitoring, moving beyond cloud-centric remote sensing
631 workflows. Low Earth Orbit (LEO) satellite constellations provide high-revisit, high-resolution

632 observations that improve small-scale canopy disturbance detections. Recent studies using
633 Planet NICFI and PlanetScope imagery show that fine-resolution observations improve tropical
634 forest cover mapping during short-duration disturbance events. (Wagner et al.,
635 2023)(Pickering et al., 2021) (Dalagnol, Hubert, et al., 2023). In the future, AI-on-chip edge
636 computing, where inference is performed close to the sensor and not only in the cloud, can be
637 explored. These systems support low-latency, low-power, and communication-efficient
638 surveillance in remote forests. (Andreadis et al., 2021)(Mporas et al., n.d.). This indicates that
639 future systems will rely on integrated architectures that combine wide-area satellite
640 surveillance with localised edge intelligence.

641 **8.2 Integration with Governance and Policy Frameworks:**

642 This study explains how the government and the courts, working together, can help companies
643 become more responsible. It introduces a concept called Government-Court Coordination
644 (GCC) which means governments help with policies and support, and courts handle legal
645 processes. This leads to reduced financial pressure for companies and better human capital.
646 This concept was implemented in China and is mainly used for bankruptcy cases. India utilises
647 remote sensing through the Forest Survey of India (FSI) to assess forest cover and monitor
648 degradation every two years. National Forest Policy (NFP) in 1988 aims to maintain 33% of
649 the geographical area under forest cover. Green India Mission (GIM) aims to increase
650 forest/tree cover by 5 million hectares (mha) and improve the quality in another 5 mha. The
651 National Compensatory Afforestation Fund Management and Planning Authority (*NATIONAL*
652 *CAMPA*) mandates the utilisation of funds for reforestation when forests are diverted for
653 industrial use.(Zhong, Qin, et al., 2026). The Indian government introduced the Forest
654 (Conservation) Amendment Act, 2023, for better forest protection. India aims to achieve Net
655 Zero carbon emission by 2070 through better forest protection. The government plans to
656 increase forest and tree cover to one-third of India's land area. The Act supports forest

657 restoration, ecological security, and sustainable development.(The Gazette of India, 2023,
658 Section 2, Preamble)

659

660 9. Conclusion

661 This review article provides a systematic overview of deforestation change detection using
662 remote sensing by evaluating key elements, including data sources, levels of analysis,
663 algorithmic techniques, and change detection outputs. The findings indicate that combining bi-
664 temporal and multi-temporal satellite imagery with advanced ML and DL models, such as
665 CNNs, U-Net variants, Transformers, and hybrid frameworks, improves detection accuracy and
666 spatiotemporal detail. Current research is still dominated by binary classification due to its
667 simplicity and efficiency, whereas multiclass approaches, though more challenging, offer
668 greater ecological interpretability. In addition, multi-source data fusion, pixel-object hybrid
669 strategies, and attention-based or self-supervised methods have contributed to notable
670 improvements in change-mapping performance across different landscape types. ML models
671 achieve high accuracy, but performance varies across studies. DL models generally show
672 higher and more consistent performance than ML models. Basic DL models achieve moderate
673 accuracy from 78% to 98% in change detection tasks. Advanced DL models like transformer
674 achieve very high performance nearly 99.79% overall accuracy and 99.15% of F1-score and
675 better feature representation. Combining advanced DL with multi-source data clearly improves
676 overall detection performance. However, important challenges remain, including limited model
677 generalizability, complex preprocessing requirements, class imbalance, scalability constraints,
678 and high computational cost. A general problem is that training the model in one region may
679 not work well in other regions or datasets. Due to data limitations, high-performing DL models
680 need large, labelled datasets, which are not always available. In terms of computational cost,
681 advanced models require high memory, longer training time and powerful GPUs. Future

682 research should therefore place greater emphasis on cross-regional generalisation and domain
683 adaptation, so that models can be transferred more reliably across ecosystems and sensor
684 settings. Real-time and near-real-time monitoring systems should also be designed to balance
685 rapid alert generation with verification reliability. Standardised benchmark datasets are needed
686 for multiclass and multimodal evaluation. Future monitoring systems will be scalable as they
687 will combine lightweight edge-deployable models with emerging technologies such as LEO
688 constellations. Future research will depend not only on higher accuracy but also on the
689 development of monitoring frameworks that are robust and operationally practical.

690

691 **References**

692 Adarme, M. O., Feitosa, R. Q., Happ, P. N., Almeida, C. A. De, & Gomes, A. R. (2020).

693 Evaluation of deep learning techniques for deforestation detection in the brazilian
694 amazon and cerrado biomes from remote sensing imagery. *Remote Sensing*, *12*(6).

695 <https://doi.org/10.3390/rs12060910>

696 Alshehri, M., Ouadou, A., Scott, G. J., & Member, S. (2024). Deep Transformer-Based

697 Network Deforestation Detection in the Brazilian Amazon Using Sentinel-2 Imagery.

698 *IEEE Geoscience and Remote Sensing Letters*, *21*(D1), 1–5.

699 <https://doi.org/10.1109/LGRS.2024.3355104>

700 Andreadis, A., Giambene, G., & Zambon, R. (2021). *Monitoring Illegal Tree Cutting through*

701 *Ultra-Low-Power Smart IoT Devices*.

702 Arcanjo, J. S., Luz, E. F. P., Fazenda, Á. L., & Ramos, F. M. (2016). Methods for evaluating

703 volunteers' contributions in a deforestation detection citizen science project. *Future*

704 *Generation Computer Systems*, *56*, 550–557.

705 <https://doi.org/10.1016/j.future.2015.07.005>

- 706 Atef, I., Ahmed, W., & Abdel-Maguid, R. H. (2023). Modelling of land use land cover
707 changes using machine learning and GIS techniques: a case study in El-Fayoum
708 Governorate, Egypt. *Environmental Monitoring and Assessment*, 195(6).
709 <https://doi.org/10.1007/s10661-023-11224-7>
- 710 Ball, J. G. C., Petrova, K., Coomes, D. A., & Flaxman, S. (2022). Using deep convolutional
711 neural networks to forecast spatial patterns of Amazonian deforestation. *Methods in
712 Ecology and Evolution*, 13(11), 2622–2634. <https://doi.org/10.1111/2041-210X.13953>
- 713 Bergamasco, L., Saha, S., Bovolo, F., & Bruzzone, L. (2022). Unsupervised Change
714 Detection Using Convolutional-Autoencoder Multiresolution Features. *IEEE
715 Transactions on Geoscience and Remote Sensing*, 60, 1–19.
716 <https://doi.org/10.1109/TGRS.2022.3140404>
- 717 Beyer, J. F., Köthke, M., & Lippe, M. (2025). *Assessing the Suitability of Available Global
718 Forest Maps as Reference Tools for EUDR-Compliant Deforestation Monitoring*. 1–28.
- 719 Boehm, H. D. V., Liesenberg, V., & Limin, S. H. (2013). Multi-temporal airborne LiDAR-
720 survey and field measurements of tropical peat swamp forest to monitor changes. *IEEE
721 Journal of Selected Topics in Applied Earth Observations and Remote Sensing*, 6(3),
722 1524–1530. <https://doi.org/10.1109/JSTARS.2013.2258895>
- 723 Brovelli, M. A., Sun, Y., & Yordanov, V. (2020). Monitoring forest change in the amazon
724 using multi-temporal remote sensing data and machine learning classification on Google
725 Earth Engine. *ISPRS International Journal of Geo-Information*, 9(10), 1–21.
726 <https://doi.org/10.3390/ijgi9100580>
- 727 Cazzolla, R., Cort, R. B., & Torresani, M. (2025). *An early warning system based on machine
728 learning detects huge forest loss in Ukraine during the war*. 58(January).
729 <https://doi.org/10.1016/j.gecco.2025.e03427>

730 Chen, W., Flatnes, J. E., Miteva, D. A., & Klaiber, H. A. (2022). The Impact of Deforestation
731 on Nature-Based Recreation: Evidence from Citizen Science Data in Mexico. *Land*
732 *Economics*, 98(1), 22–40. <https://doi.org/10.3368/le.98.1.031020-0036r1>

733 Cheng, G., Huang, Y., Li, X., Lyu, S., Xu, Z., & Zhao, H. (2024). *Change Detection Methods*
734 *for Remote Sensing in the Last Decade : A Comprehensive Review*. 1–36.

735 Cherif, E., Hell, M., & Brandmeier, M. (2022). DeepForest: Novel Deep Learning Models for
736 Land Use and Land Cover Classification Using Multi-Temporal and -Modal Sentinel
737 Data of the Amazon Basin. *Remote Sensing*, 14(19). <https://doi.org/10.3390/rs14195000>

738 Coțolan, L., & Moldovan, D. (2024). Applicability of pre-trained CNNs in temperate
739 deforestation detection ABSTRACT. *European Journal of Remote Sensing*, 57(1).
740 <https://doi.org/10.1080/22797254.2024.2367221>

741 Dalagnol, R., Hubert, F., Galv, S., Braga, D., Payne, M., Osborn, F., Sagang, L. B., Silva, C.,
742 Favrichon, S., Silgueiro, V., & Anderson, L. O. (2023). *Remote Sensing of Environment*
743 *Mapping tropical forest degradation with deep learning and Planet NICFI data*.
744 298(August). <https://doi.org/10.1016/j.rse.2023.113798>

745 Dalagnol, R., Wagner, F. H., Galvão, L. S., Braga, D., Osborn, F., Sagang, L. B., da
746 Conceição Bispo, P., Payne, M., Silva Junior, C., Favrichon, S., Silgueiro, V., Anderson,
747 L. O., Aragão, L. E. O. e. C. de, Fensholt, R., Brandt, M., Ciais, P., & Saatchi, S. (2023).
748 Mapping tropical forest degradation with deep learning and Planet NICFI data. *Remote*
749 *Sensing of Environment*, 298. <https://doi.org/10.1016/j.rse.2023.113798>

750 de Andrade, R. B., Mota, G. L. A., & da Costa, G. A. O. P. (2022). Deforestation Detection
751 in the Amazon Using DeepLabv3+ Semantic Segmentation Model Variants. *Remote*
752 *Sensing*, 14(19). <https://doi.org/10.3390/rs14194694>

753 de Bem, P. P., de Carvalho, O. A., Guimarães, R. F., & Gomes, R. A. T. (2020). Change
754 detection of deforestation in the brazilian amazon using landsat data and convolutional
755 neural networks. *Remote Sensing*, *12*(6). <https://doi.org/10.3390/rs12060901>

756 Desclée, B., Simonetti, D., Mayaux, P., & Achard, F. (2013). Multi-sensor monitoring system
757 for forest cover change assessment in central africa. *IEEE Journal of Selected Topics in*
758 *Applied Earth Observations and Remote Sensing*, *6*(1), 110–120.
759 <https://doi.org/10.1109/JSTARS.2013.2240263>

760 Doblas, J., Reis, M. S., Belluzzo, A. P., Quadros, C. B., Moraes, D. R. V, Almeida, C. A.,
761 Maurano, L. E. P., Carvalho, A. F. A., Anna, S. J. S. S., & Shimabukuro, Y. E. (2022).
762 *DETER-R : An Operational Near-Real Time Tropical Forest Disturbance Warning*
763 *System Based on Sentinel-1 Time Series Analysis*. 1–21.

764 Dong, H., Ma, W., Member, S., & Jiao, L. (2024). Contrastive Learning With Context-
765 Augmented Transformer for Change Detection in SAR Images. *IEEE Journal of*
766 *Selected Topics in Applied Earth Observations and Remote Sensing*, *17*, 17710–17724.
767 <https://doi.org/10.1109/JSTARS.2024.3464735>

768 Durowoju, O. S. (2025). Urban change detection : assessing biophysical drivers using
769 machine learning and Google Earth Engine. *Environmental Monitoring and Assessment*.
770 <https://doi.org/10.1007/s10661-025-13863-4>

771 Farhadpour, S., Warner, T. A., & Maxwell, A. E. (2024). *Selecting and Interpreting*
772 *Multiclass Loss and Accuracy Assessment Metrics for Classifications with Class*
773 *Imbalance : Guidance and Best Practices*. 1–22.

774 Fodor, G., & Conde, M. V. (2023). *Rapid Deforestation and Burned Area Detection using*
775 *Deep Multimodal Learning on Satellite Imagery*. <http://arxiv.org/abs/2307.04916>

- 776 Gupta, L., Dixit, J., Chandra, P., & Manish, P. (2025). Assessment of forest cover dynamics
777 for the detection of deforestation in the Hindu Kush Himalayan region using geospatial
778 and machine learning approaches. In *Earth Science Informatics*. Springer Berlin
779 Heidelberg. <https://doi.org/10.1007/s12145-024-01517-x>
- 780 Gupta, N., Ari, S., & Panigrahi, N. (2021). Change detection in landsat images using
781 unsupervised learning and RBF-based clustering. *IEEE Transactions on Emerging*
782 *Topics in Computational Intelligence*, 5(2), 284–297.
783 <https://doi.org/10.1109/TETCI.2019.2932087>
- 784 Hansen, J. N., Mitchard, E. T. A., & King, S. (2020). Assessing forest/non-forest separability
785 using sentinel-1 C-band synthetic aperture radar. *Remote Sensing*, 12(11).
786 <https://doi.org/10.3390/rs12111899>
- 787 Hansen, M. C., Potapov, P. V., Moore, R., Hancher, M., Turubanova, S. A., Tyukavina, A.,
788 Thau, D., Stehman, S. V., Goetz, S. J., Loveland, T. R., Kommareddy, A., Egorov, A.,
789 Chini, L., Justice, C. O., & Townshend, J. R. G. (2013). High-resolution global maps of
790 21st-century forest cover change. *Science*, 342(6160), 850–853.
791 <https://doi.org/10.1126/science.1244693>
- 792 Haq, N. ul, Rahman, F., Tabassum, I., & Mehran. (2021). Forest cover dynamics in Palas
793 Valley Kohistan, Hindu Kush-Himalayan Mountains, Pakistan. *Journal of Mountain*
794 *Science*, 18(2), 416–426. <https://doi.org/10.1007/s11629-020-6093-4>
- 795 Javed, A., Kim, T., Lee, C., Oh, J., & Han, Y. (2023). Deep Learning-Based Detection of
796 Urban Forest Cover Change along with Overall Urban Changes Using Very-High-
797 Resolution Satellite Images. *Remote Sensing*, 15(17).
798 <https://doi.org/10.3390/rs15174285>
- 799 John, D., & Zhang, C. (2022). An attention-based U-Net for detecting deforestation within

800 satellite sensor imagery. *International Journal of Applied Earth Observation and*
801 *Geoinformation*, 107(January), 102685. <https://doi.org/10.1016/j.jag.2022.102685>

802 Karishma, C. G., Kannan, B., Nagarajan, K., Panneerselvam, S., & Pazhanivelan, S. (2022).
803 Land use land cover change detection in the lower Bhavani basin, Tamil Nadu, using
804 geospatial techniques. *Journal of Applied and Natural Science*, 14(SI), 58–64.
805 <https://doi.org/10.31018/jans.v14iSI.3566>

806 Karmoude, Y., Idbraim, S., Saidi, S., & Masse, A. (2025). *Efficient Argan Tree Deforestation*
807 *Detection Using Sentinel-2 Time Series and Machine Learning*.

808 Kushwaha, M. (2025). ScienceDirect Enhancing Forest Image Segmentation in Aerial Images
809 using Deep Enhancing Forest Image Segmentation Learning in Aerial Images using
810 Deep Learning. *Procedia Computer Science*, 258, 2760–2766.
811 <https://doi.org/10.1016/j.procs.2025.04.536>

812 Laurance, W. F., Clements, G. R., Sloan, S., O’Connell, C. S., Mueller, N. D., Goosem, M.,
813 Venter, O., Edwards, D. P., Phalan, B., Balmford, A., Van Der Ree, R., & Arrea, I. B.
814 (2014). A global strategy for road building. *Nature*, 513(7517), 229–232.
815 <https://doi.org/10.1038/nature13717>

816 Lee, D., & Choi, Y. (2023). A Learning Strategy for Amazon Deforestation Estimations
817 Using Multi-Modal Satellite Imagery. *Remote Sensing*, 15(21).
818 <https://doi.org/10.3390/rs15215167>

819 Li, X., Xie, W., Member, S., Zhang, J., & Li, Y. (2025). CMCD : A Consistency Model-
820 Based Change Detection Method for Remote Sensing Images. *IEEE Journal of Selected*
821 *Topics in Applied Earth Observations and Remote Sensing*, 18, 9009–9022.
822 <https://doi.org/10.1109/JSTARS.2025.3554659>

- 823 Li, Y., Li, S., Xu, X., Wu, Z., & Fan, H. (2025). International Journal of Applied Earth
824 Observation and Geoinformation A novel topographic correction framework for
825 detecting forest disturbance from annual wide-time-window Landsat time series.
826 *International Journal of Applied Earth Observation and Geoinformation*, 139(2),
827 104568. <https://doi.org/10.1016/j.jag.2025.104568>
- 828 Liu, Q., Luo, X., & Su, M. (2024). *Analysis of the "Greenwashing" Phenomenon in the ESG*
829 *Investment Environment*. 40, 1161–1170.
- 830 Lucas, R. M., Lee, A. C., & Williams, M. L. (2006). Enhanced simulation of radar
831 backscatter from forests using LiDAR and optical data. *IEEE Transactions on*
832 *Geoscience and Remote Sensing*, 44(10), 2736–2754.
833 <https://doi.org/10.1109/TGRS.2006.881802>
- 834 Ma, S. (2025). *Clear Waters , Flourishing Growth : Decoupling Water Pollution From*
835 *Economic Growth in Shanxi*. <https://doi.org/10.1002/wer.70231>
- 836 Ma, S., Liu, H., Zeng, H., Li, D., & Yan, H. (2026). From Loom to Algorithm : How Digital
837 Technologies Drive Quality Development in the Textile Sector From Loom to
838 Algorithm : How Digital Technologies Drive Quality Development in the Textile Sector.
839 *The Journal of The Textile Institute*, 0(0), 1–17.
840 <https://doi.org/10.1080/00405000.2026.2622882>
- 841 Masolele, R. N., De Sy, V., Herold, M., Marcos Gonzalez, D., Verbesselt, J., Gieseke, F.,
842 Mullissa, A. G., & Martius, C. (2021). Spatial and temporal deep learning methods for
843 deriving land-use following deforestation: A pan-tropical case study using Landsat time
844 series. *Remote Sensing of Environment*, 264(May), 112600.
845 <https://doi.org/10.1016/j.rse.2021.112600>
- 846 Masolele, R. N., De Sy, V., Marcos, D., Verbesselt, J., Gieseke, F., Mulatu, K. A., Moges,

847 Y., Sebrala, H., Martius, C., & Herold, M. (2022). Using high-resolution imagery and
848 deep learning to classify land-use following deforestation: a case study in Ethiopia.
849 *GIScience and Remote Sensing*, 59(1), 1446–1472.
850 <https://doi.org/10.1080/15481603.2022.2115619>

851 Maxwell, A. E., & Warner, T. A. (2026). *Accuracy Assessment in Convolutional Neural*
852 *Network-Based Deep Learning Remote Sensing Studies — Part 2 : Recommendations*
853 *and Best Practices.*

854 Meiaraj, N. G. S. and C. (2025). *Land use and land cover change detection by machine*
855 *learning classi B ers (SVM and RF) using satellite remote sensing observations for*
856 *Cuddalore Taluk , Tamil Nadu , India.* 22. <https://doi.org/10.1007/s12040-024-02484-z>

857 Messias, C. G., Almeida, C. A. De, Silva, D. E., Soler, L. S., Maurano, L. E., Camilotti, V.
858 L., Alves, F. C., Silva, L. J., Reis, M. S., Lima, T. C. De, Renó, V., Lima, D. L. C.,
859 Belluzzo, A. P., Quadros, C. B., Barradas, D. C. M., Moraes, D. R. V. De, Bastos, E. F.
860 M., Cunha, I. P., Souza, J. J. De, ... Matos, A. P. (2024). Unaccounted for nonforest
861 vegetation loss in the Brazilian Amazon. *Communications Earth & Environment.*
862 <https://doi.org/10.1038/s43247-024-01542-0>

863 Moni, J., Subrata, B., Hitendra, N., Rocky, P., Arun, P., & Nath, J. (2025). *Harnessing Time-*
864 *Series Satellite Data and Deep Learning to Monitor Historical Patterns of Deforestation*
865 *in Eastern Himalayan Foothills of.* 993–1008.

866 Mporas, I., Perikos, I., & Kelefouras, V. (n.d.). *applied sciences Illegal Logging Detection*
867 *Based on Acoustic Surveillance of Forest.*

868 Neves, C. N., Feitosa, R. Q., Adarme, M. X. O., & Giraldi, G. A. (2023). *Combining*
869 *recurrent and residual learning for deforestation monitoring using multitemporal SAR*
870 *images.* <http://arxiv.org/abs/2310.05697>

- 871 Nguyen Trong, H., Nguyen, T. D., & Kappas, M. (2020). Land Cover and Forest Type
872 Classification by Values of Vegetation Indices and Forest Structure of Tropical Lowland
873 Forests in Central Vietnam. *International Journal of Forestry Research*, 2020.
874 <https://doi.org/10.1155/2020/8896310>
- 875 Nyamtseren, M., Pham, T. D., Thi, T., Vu, P., Navaandorj, I., & Shoyama, K. (2025).
876 *Mapping Vegetation Changes in Mongolian Grasslands (1990 – 2024) Using Landsat*
877 *Data and Advanced Machine Learning Algorithm*. 1–17.
- 878 Oca, A. I. F. De, Ghilardi, A., Kauffer, E., Mas, J. F., Sánchez-cordero, V., & Gallardo-cruz,
879 J. A. (2025). *Building a Methodological Reference Framework for Quantifying Tropical*
880 *Deforestation with Remote Sensing*. 1–18.
- 881 Pacheco-Pascagaza, A. M., Gou, Y., Louis, V., Roberts, J. F., Rodríguez-Veiga, P., Bispo, P.
882 da C., Espírito-Santo, F. D. B., Robb, C., Upton, C., Galindo, G., Cabrera, E., Cendales,
883 I. P. P., Santiago, M. A. C., Negrete, O. C., Meneses, C., Iñiguez, M., & Balzter, H.
884 (2022). Near Real-Time Change Detection System Using Sentinel-2 and Machine
885 Learning: A Test for Mexican and Colombian Forests. *Remote Sensing*, 14(3), 1–21.
886 <https://doi.org/10.3390/rs14030707>
- 887 Pickering, J., Tyukavina, A., Khan, A., Potapov, P., Adusei, B., & Hansen, M. C. (2021).
888 *Using Multi-Resolution Satellite Data to Quantify Land Dynamics : Applications of*
889 *PlanetScope Imagery for Cropland and Tree-Cover Loss Area Estimation*.
- 890 Potić, I., Srdić, Z., Vakanjac, B., Bakrač, S., Đorđević, D., Banković, R., & Jovanović, J. M.
891 (2023). Improving Forest Detection Using Machine Learning and Remote Sensing: A
892 Case Study in Southeastern Serbia. *Applied Sciences (Switzerland)*, 13(14).
893 <https://doi.org/10.3390/app13148289>
- 894 Pulella, A., Santos, R. A., Sica, F., Posovszky, P., & Rizzoli, P. (2020). Multi-temporal

895 sentinel-1 backscatter and coherence for rainforest mapping. *Remote Sensing*, 12(5), 1–
896 17. <https://doi.org/10.3390/rs12050847>

897 Rakshit, S., Debnath, S., & Mondal, D. (2018). *Identifying land patterns from satellite*
898 *imagery in amazon rainforest using deep learning*. arXiv preprint arXiv:1809.00340.

899 Rash, A., Mustafa, Y., & Hamad, R. (2023). Quantitative assessment of Land use/land cover
900 changes in a developing region using machine learning algorithms: A case study in the
901 Kurdistan Region, Iraq. *Heliyon*, 9(11). <https://doi.org/10.1016/j.heliyon.2023.e21253>

902 Reading, I., Bika, K., Drakesmith, T., McNeill, C., Cheesbrough, S., Byrne, J., & Balzter, H.
903 (2024). *Due Diligence for Deforestation-Free Supply Chains with Copernicus Sentinel-2*
904 *Imagery and Machine Learning*. 1–20.

905 Richardson, G., Knudby, A., Crowley, M. A., Sawada, M., Richardson, G., Knudby, A.,
906 Crowley, M. A., & Sawada, M. (2025). Machine learning approaches to Landsat change
907 detection analysis. *Canadian Journal of Remote Sensing*, 51(1).
908 <https://doi.org/10.1080/07038992.2024.2448169>

909 Selvaraj, R., & Amali, D. G. B. (2023). Assessment of object-based classification for
910 mapping land use and land cover using google earth. *Global Nest Journal*, 25(7), 131–
911 138. <https://doi.org/10.30955/gnj.004829>

912 Selvaraj, R., & Amali D, G. B. (2023). Accurate classification of land use and land cover
913 using a boundary-specific two-level learning approach augmented with auxiliary
914 features in Google Earth Engine. *Environmental Monitoring and Assessment*, 195(11).
915 <https://doi.org/10.1007/s10661-023-11903-5>

916 Somnath Rakshit., et al. (2018). *Identifying Land Patterns from Satellite Imagery in Amazon*
917 *Rainforest using Deep Learning*. 1–5.

918 Soto, P. J., Costa, G. A., Feitosa, R. Q., Ortega, M. X., Bermudez, J. D., & Turnes, J. N.
919 (2022). Domain-Adversarial Neural Networks for Deforestation Detection in Tropical
920 Forests. *IEEE Geoscience and Remote Sensing Letters*, 19.
921 <https://doi.org/10.1109/LGRS.2022.3163575>

922 Soto Vega, P. J., Costa, G. A. O. P. da, Feitosa, R. Q., Ortega Adarme, M. X., Almeida, C. A.
923 de, Heipke, C., & Rottensteiner, F. (2021). An unsupervised domain adaptation
924 approach for change detection and its application to deforestation mapping in tropical
925 biomes. *ISPRS Journal of Photogrammetry and Remote Sensing*, 181(September), 113–
926 128. <https://doi.org/10.1016/j.isprsjprs.2021.08.026>

927 Srivastava, S., & Ahmed, T. (2024). DLCD : Deep learning-based change detection approach
928 to monitor deforestation. *Signal, Image and Video Processing*, 18.
929 <https://doi.org/10.1007/s11760-024-03140-1>

930 Tarazona, Y., Zabala, A., Pons, X., Broquetas, A., Nowosad, J., & Zurqani, H. A. (2021).
931 Fusing Landsat and SAR Data for Mapping Tropical Deforestation through Machine
932 Learning Classification and the PVts- β Non-Seasonal Detection Approach. *Canadian*
933 *Journal of Remote Sensing*, 47(5), 677–696.
934 <https://doi.org/10.1080/07038992.2021.1941823>

935 Torres, D. L., Turnes, J. N., Vega, P. J. S., Feitosa, R. Q., Silva, D. E., Marcato Junior, J., &
936 Almeida, C. (2021). Deforestation detection with fully convolutional networks in the
937 amazon forest from landsat-8 and sentinel-2 images. *Remote Sensing*, 13(24), 1–20.
938 <https://doi.org/10.3390/rs13245084>

939 Vega, P. J. S., Da Costa, G. A. O. P., Adarme, M. X. O., Castro, J. D. B., & Feitosa, R. Q.
940 (2023). Weakly Supervised Domain Adversarial Neural Network for Deforestation
941 Detection in Tropical Forests. *IEEE Journal of Selected Topics in Applied Earth*

942 *Observations and Remote Sensing*, 16, 10264–10278.
943 <https://doi.org/10.1109/JSTARS.2023.3327573>

944 Wagner, F. H., Dalagnol, R., Silva-Junior, C. H. L., Carter, G., Ritz, A. L., Hirye, M. C. M.,
945 Ometto, J. P. H. B., & Saatchi, S. (2023). Mapping Tropical Forest Cover and
946 Deforestation with Planet NICFI Satellite Images and Deep Learning in Mato Grosso
947 State (Brazil) from 2015 to 2021. *Remote Sensing*, 15(2).
948 <https://doi.org/10.3390/rs15020521>

949 Wang, Z., Liu, D., Liao, X., Pu, W., Wang, Z., & Zhang, Q. (2023). SiamHRnet-OCR: A
950 Novel Deforestation Detection Model with High-Resolution Imagery and Deep
951 Learning. *Remote Sensing*, 15(2). <https://doi.org/10.3390/rs15020463>

952 Welsink, A., Reiche, J., Sy, V. De, Carter, S., & Slagter, B. (2023). *Towards the use of*
953 *satellite-based tropical forest disturbance alerts to assess selective logging intensities*
954 *OPEN ACCESS Towards the use of satellite-based tropical forest disturbance alerts to*
955 *assess selective logging intensities.*

956 Wu, H., Cui, T., & Cao, L. (2025). *Simultaneous Reductions in Forest Resilience and*
957 *Greening Trends in Southwest China.* 1–30.

958 Xu, C., Yao, X., Yan, H., & Li, Y. (2025). *Does ESG Disclosure Improve Green Innovation*
959 *Performance of New Energy Enterprises ? Evidence from China.* 34(4), 4859–4868.
960 <https://doi.org/10.15244/pjoes/190649>

961 Xu, K., Qian, J., Hu, Z., Duan, Z., Chen, C., Liu, J., Sun, J., Wei, S., & Xing, X. (2021). A
962 new machine learning approach in detecting the oil palm plantations using remote
963 sensing data. *Remote Sensing*, 13(2), 1–17. <https://doi.org/10.3390/rs13020236>

964 Yan, H., Yao, X., Li, Y., & Xiong, Z. (2025). *Capital market liberalization and corporate*

965 *ESG rating divergence : a quasi-natural experiment based on the trading system of*
966 *SSHC. 57(60), 11107–11121.*

967 Zeng, H., Liu, H., Yan, H., & Ma, S. (2025). Borsa Istanbul Review Biodiversity risk and
968 global stock markets : A cross-national heterogeneity analysis based on quantile-on-
969 quantile methods. *Borsa Istanbul Review, 25(6)*, 1518–1529.
970 <https://doi.org/10.1016/j.bir.2025.10.013>

971 Zerrouki, Y., Harrou, F., Zerrouki, N., Dairi, A., & Sun, Y. (2021). Desertification Detection
972 Using an Improved Variational Autoencoder-Based Approach through ETM-Landsat
973 Satellite Data. *IEEE Journal of Selected Topics in Applied Earth Observations and*
974 *Remote Sensing, 14*, 202–213. <https://doi.org/10.1109/JSTARS.2020.3042760>

975 Zhang, X., Su, H., Zhang, C., Gu, X., Tan, X., & Atkinson, P. M. (2021). Robust
976 unsupervised small area change detection from SAR imagery using deep learning.
977 *ISPRS Journal of Photogrammetry and Remote Sensing, 173*(December 2020), 79–94.
978 <https://doi.org/10.1016/j.isprsjprs.2021.01.004>

979 Zhang, Y., Song, X., Hua, Z., & Li, J. (2024). CGMMA: CNN-GNN Multiscale Mixed
980 Attention Network for Remote Sensing Image Change Detection. *IEEE Journal of*
981 *Selected Topics in Applied Earth Observations and Remote Sensing, 17(8)*, 7089–7103.
982 <https://doi.org/10.1109/JSTARS.2024.3358298>

983 Zheng, D., Wu, Z., Member, S., & Liu, J. (2024). Detail Enhanced Change Detection in VHR
984 Images Using a Self-Supervised Multiscale Hybrid Network. *IEEE Journal of Selected*
985 *Topics in Applied Earth Observations and Remote Sensing, 17*, 3181–3196.
986 <https://doi.org/10.1109/JSTARS.2023.3348630>

987 Zhong, Y., Qin, B., Liu, Z., & Yan, H. (2026). *Coordinating bankruptcy reform :*
988 *Government – court collaboration and firm innovation through financial and human*

989 *capital channels*. 91(March), 372–391.

990 Zhong, Y., Yan, H., & Xia, Z. (2026). Technology in Society Who is lifting the green veil ?

991 Climate physical risks and supply chain spillovers of corporate carbon greenwashing.

992 *Technology in Society*, 85(December 2025), 103203.

993 <https://doi.org/10.1016/j.techsoc.2025.103203>

994 Zhou, Y., Li, X., Chen, K., & Kung, S. Y. (2023). Progressive Learning for Unsupervised

995 Change Detection on Aerial Images. *IEEE Transactions on Geoscience and Remote*

996 *Sensing*, 61. <https://doi.org/10.1109/TGRS.2023.3235981>

997 Zhou, Z., Zheng, C., Liu, X., Tian, Y., Chen, X., Chen, X., & Dong, Z. (2023). *A Dynamic*

998 *Effective Class Balanced Approach for Remote Sensing Imagery Semantic Segmentation*

999 *of Imbalanced Data*.

1000 The Gazette of India. (2023). *The Forest (Conservation) Amendment Act, 2023 (No. 15 of*

1001 *2023)*. Ministry of Law and Justice, Government of India.

1002